 SDHM, vol.7, no.1, pp.23-64, 2011

Structural Damage Detection using Spatial Fourier Coefficients of Mode Shapes of Beams Simply Supported at Both Ends

Gouravaraju Saipraneeth[1] **and Ranjan Ganguli**[2]

Abstract: In this paper, the effect of damage on mode shape related parameters of a beam is investigated. The damage is represented by a localized reduction in beam stiffness. The damage location and amount is varied using a finite element model of the beam to obtain the mode shapes. A beam which is simply supported at both ends is used for the numerical results. The periodic nature of the beam is exploited to obtain spatial Fourier coefficients of the mode shapes. As the damage location and size are varied, it is found that the Fourier coefficients also change and are found to be sensitive to damage location and size. Even in the presence of noise, Fourier coefficients are found to be effective in indicating the damage.

Keywords: Beam, Damage, Finite Element Model, Fourier Analysis, Mode Shapes, Noise.

Nomenclature

a_i, b_j = Fourier coefficients

D = Continuum damage variable

E = Young's modulus

I = Area moment of inertia of the beam cross-section

K = Stiffness matrix

[1] Research Assistant, E-mail: gouravaraju@gmail.com

[2] Professor, Corresponding Author, Indian Institute of Science, Bangalore, Email: ganguli@aero.iisc.ernet.in, http://aero.iisc.ernet.in/ganguli, Tel: 91-80-22933017, Fax:91-80-23600134

L = Length of the beam

m = Mass per unit length of the beam

M = Mass matrix

n = Number of dof in FE model

p = Period in spatial domain

q = Vector of nodal dofs

$w = w(x,t)$ = Transverse displacement of the beam

W = Modal transverse displacement

x = Length measured along the axis of the beam

β_i = i^{th} root of frequency equation

Φ = Mode shape vector

η = Linear transformation = $\frac{2\pi x}{L}$

ρ = Uniform mass density

ω = Natural frequency

α = Noise level parameter.

1 Introduction

Structural damage detection is a widely researched area(Yana, Cheng, Wu, Yam (2007), Carden, Fanning (2004), Zou, Tong, Steven (2000) and Doebling, Farrar, Prime (1998)). Many damage detection techniques have been developed to monitor the changes in the structure's characteristics caused by factors such as environmental effects, repetitive loading and aging of the structure etc. At present,

Nondestructive Damage Detection (NDD) is the widely used method. Techniques like ultrasonics, radiography, CT scanning and eddy current are used for detecting local damage in structures. These methods can be applied effectively for small and accessible portions of a large structure. Hence these methods are called “local" NDD methods (Yoon, Heider, Gillespie, Ratcliffe and Crane (2005)). However, for large and complicated structures, these methods cannot be applied to detect damage. Therefore, the limited application of local NDD methods led to the development of global damage detection techniques based on vibration analysis. These methods can be applied to the large and complex structures. The basic principle in these vibration analysis methods is as follows. The dynamic characteristics of a structure such as natural frequency and mode shapes are effected by the changes in the structural parameters like mass, stiffness and damping. These variations in dynamic characteristics are obtained using different methods and often subjected to signal processing or a transformation before being used for detecting the damage in the structure.

The vibration based damage detection methods are mainly based on two dynamic characteristics: natural frequency and mode shapes. The ease of measuring and its accuracy makes the methods which use changes in natural frequency very advantageous. A few recent studies on the use of natural frequency in damage detection are discussed next. Zhong, Oyadiji and Ding (2008) used the response time history of beam like structures and auxiliary mass space probing to enhance the effects of damage in the beam. As the auxiliary mass travels along the beam, the natural frequency of the beam changes due to change in the inertia and variation in the flexibility of the beam. It was shown that it is difficult to locate the crack directly from the curves drawn between modal frequencies obtained by the spectral centre correction method (SCCM) versus the location of auxiliary mass. So, they proposed a method which uses derivatives of natural frequency curves for damage detection. Wang and He (2007) performed simulation and experiments on a hypothetical concrete dam for crack detection by monitoring the reduction in natural frequencies. They proposed a statistical neural network which detects changes in the natural frequencies. Despite its advantages in terms of simplicity, the frequency based method often fails to be sensitive to initial and small damage. Zhao, Tang and Wang (2007) tried to overcome this problem by using the tunable piezoelectric transducer circuitry which enhances the frequency changes under uncertainty and noise. They formulated a statistical damage identification algorithm which can identify both the mean and variance of the elemental property change.

The variation in mode shapes caused by damage is the key for many works done in the field of non-destructive damage detection. These works use different kinds of methodology to enhance the changes in mode shapes due to a localized damage.

Pandey, Biswas and Samman (1991) used curvature of mode shapes as a potential damage indicator. Ratcliffe (1997) used the Laplacian of the mode shape of a damaged beam. These curvature based methods involve numerical differentiation of the measured data, but are more effective in finding small defects in beams. However, Hong, Kim, Lee and Lee (2002) point out that numerical derivatives are prone to errors when measured data are noisy. However, newer instrumentation such as laser doppler vibrometers (LDV) permit a very high degree of sampling and high precision measurement of mode shapes (Sazonov, Klinkhachorn (2005)). Also, digital imaging methods are now available, making the spatial resolution of mode shapes better (Poudel, Fu and Ye (2005)). Therefore, mode shape based methods are becoming a more realistic choice in damage detection. In fact, some recent research advocates the use of third and fourth order derivatives of the mode shapes for damage detection (Whalen (2008)).

Research continues on the creation of new methods to amplify the effect of damage on the mode shapes. Reddy and Ganguli (2007) found that for a fixed-fixed beam, the spatial Fourier coefficients vary considerably with the damage location and size. Fang and Perera (2009) used power mode shapes instead of conventional mode shapes which are developed from the root mean square property of the response signal. Park, Kim, Hong, Ho and Yi (2009) used time-modal features and artificial neural networks. In this work, they used mode shapes and modal strain energies to design a modal feature-based neural networks (MBNN) algorithm which can estimate the location and severity of damage in the structure. Gokdag and Kopmaz (2009) proposed a damage detection technique based on the combination of continuous and discrete wavelet transforms. They also used mode shapes for damage detection purpose. Chandrashekhar and Ganguli (2009) proposed a method for damage detection in structures with uncertainty based on the mode-shape curvature and fuzzy logic. They used curvature damage factor (CDF) as damage indicator and Monte carlo simulations were used to study the changes in CDF. The research discussed above is a very small sample of the work done on damage detection using modal parameters. Yana, Cheng, Wu and Yam (2007) have reviewed the recent developments in vibration based damage detection techniques.

Several researchers have also looked at wavelet analysis of the mode shapes for damage detection. The wavelet transformation uses the special sets of basis which are localized both in the time and frequency domains (Poudel, Fu and Ye (2005)). Therefore, it has been argued that the local change in mode shapes are better amplified using wavelet transform. Though wavelet based approaches have been successfully demonstrated, the literature shows that the appropriate choice of wavelets is critical for successful damage detection. For instance, the Haar wavelet was used by Quek, Wang, Zhang and Ang (2001), the Mexican hat wavelet along with

the Lipschitz exponent as damage indicator by Hong, Kim, Lee and Lee (2002), a "symmetrical 4" wavelet by Douka, Louridis and Trochidis (2003), complex Gaussian wavelet by Poudel, Fu and Ye (2005), among others. The importance of the selection of appropriate wavelets adds complexity to the process of mode shape based spatial damage detection by these methods. It is thus interesting to study if the classical and well understood Fourier approach can be used for structural damage detection.

In this paper, we illustrate the use of spatial Fourier coefficients for the damage detection of periodic structures. The effect of localized damage on an Euler-Bernoulli beam which is simply supported at both ends (Fig. 1) is studied using spatial Fourier analysis. A finite element model of the beam is created and used to numerically simulate the effect of damage size and location on the mode shapes of the beam.

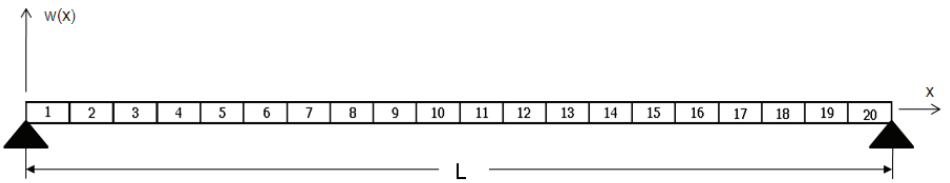

Figure 1: Typical simply supported beam discretized into 20 elements

2 Modeling of Beam

An Euler-Bernoulli beam structure is considered for damage detection in this study. The governing equation of motion for the beam is given by

$$\frac{\partial^2}{\partial x^2}\left(EI(x)\frac{\partial^2 w(x,t)}{\partial x^2}\right)+m(x)\frac{\partial^2 w(x,t)}{\partial t^2}=f(x,t) \tag{1}$$

Now considering the beam as uniform ($EI(x)=EI,\ \ m(x)=m$), one can get the exact solution by setting $f(x,t)=0$ for free vibration and assume $w(x,t)=W(x)e^{i\omega t}$. Then Eq. 1 transforms into

$$\frac{d^4W(x)}{dx^4}-\omega^2\frac{mW}{EI}=0 \tag{2}$$

The solution for the above 4^{th} order ordinary differential equation is given by

$$W(x)=C_1\cos(\lambda x)+C_2\sin(\lambda x)+C_3\cosh(\lambda x)+C_4\sinh(\lambda x) \tag{3}$$

where λ is given by

$$\lambda = \left(\frac{m\omega^2}{EI}\right)^{\frac{1}{4}} \tag{4}$$

and ω is the natural frequency.

By applying the appropriate boundary conditions and solving Eq. 3, one can get the frequency equation. There are four boundary conditions for this problem, and putting them in Eq. 3 also yields the mode shapes of the beam. Substituting the roots of this frequency equation, $(\beta)_i, (i = 1,2,.....n)$, in $\lambda = \left(\frac{m\omega^2}{EI}\right)^{\frac{1}{4}}$ where $\lambda = \frac{\beta}{L}$, we obtain the i^{th} frequency. Substituting λ in Eq. 3 gives the mode shape corresponding to the i^{th} mode.

The damage reduces the stiffness at a local level making the beam non-uniform. Using continuum damage mechanics, damage can be modeled as a localized reduction in E (Sawyer and Rao (2000)). Also, it could be considered as a reduction in I due to a localized change in geometry of the beam (Morlier, Bos and Castera (2006)). In general, a local reduction in $EI(x)$ is simple and effective approach to model damage in a beam. Numerical methods need to be used to model such non-uniform beams.

For analyzing non-uniform beams with finite element analysis, the beam is discretized into a number of elements (Fig. 1). The equation of motion for an n degree freedom system in discrete form after the assembly of the element matrices and application of the boundary conditions is given by

$$\mathbf{M}\ddot{\mathbf{q}} + \mathbf{K}\mathbf{q} = 0 \tag{5}$$

Here $\mathbf{M}$ is the $n \times n$ mass matrix of the system, $\mathbf{K}$ is the $n \times n$ stiffness matrix of the system and $\mathbf{q}$ is the $n \times 1$ vector of nodal degrees of freedom. The solution for this problem is of the form $\mathbf{q} = \Phi e^{i\omega t}$, which results in the eigenvalue problem.

$$\mathbf{K}\Phi = \omega^2\mathbf{M}\Phi \tag{6}$$

Solving this eigenvalue problem one can get n eigenvalues which represent the n natural frequencies of the system. The associated eigenvectors along with shape functions give the mode shape corresponding to that mode.

Now for a simply supported beam the boundary conditions are given by

$$W(0) = 0, W(L) = 0, \frac{d^2W(0)}{dx^2} = 0, \frac{d^2W(L)}{dx^2} = 0 \tag{7}$$

By substituting these boundary conditions in Eq. 3, and solving, one can get the frequency equation as

$$\sin(\lambda L) = 0 \tag{8}$$

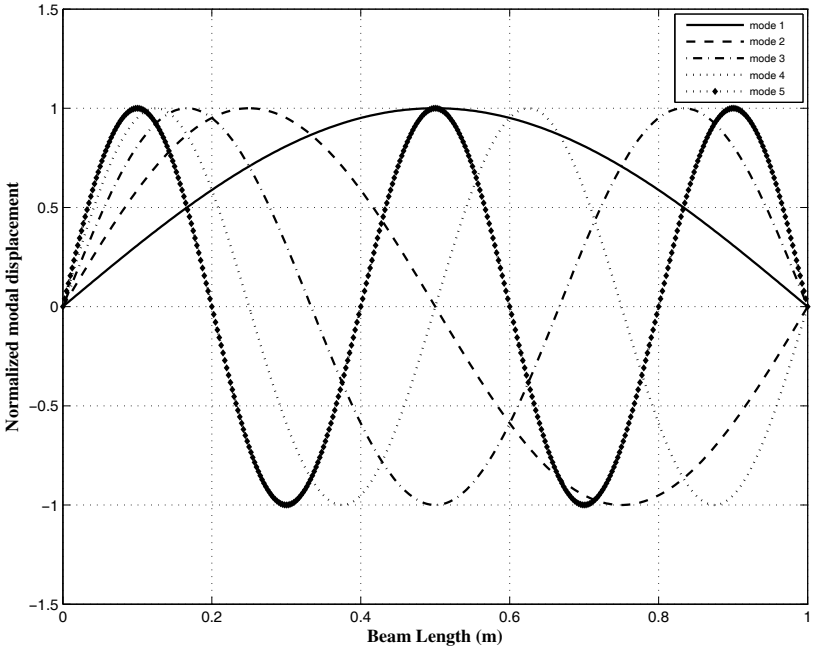

Figure 2: First Five mode shapes for an undamaged simply supported beam

The first Five roots of above equation are π, 2π, 3π, 4π, 5π respectively. Substituting these in Eq. 8 gives the corresponding mode shapes as shown in Fig. 2.

$$W(x) = \sin\left(\frac{\beta x}{L}\right) \tag{9}$$

From the Eq. 9 one can observe that mode shapes are *periodic* with $p = L$. A periodic function can be represented using a Fourier series. So, we can express the mode shapes in the form of Fourier series as in Eq. 10, taking the linear transformation $\eta = \frac{2\pi x}{L}$ which transforms the problem from $x \in [0, L]$ to $\eta \in [0, 2\pi]$

$$W(\eta) = a_0 + \sum_{i=1}^{k} \{a_i \cos(i\eta) + b_j \sin(i\eta)\} \tag{10}$$

where $a_i, (i = 1, 2, ...k)$ and $b_j, j = (1, 2, ...k)$ are Fourier coefficients. Then the mode shapes are uniformly sampled at a number of discrete points and normalized with respect to highest value. Now by fitting a curve similar to that in Eq. 9 one can get the Fourier coefficients of the mode shapes. Note that in contrast to the widespread application of Fourier analysis in the time domain, we are applying it here in the spatial domain.

3 Modeling of damage

When a damage occurs in a structure, the structural parameters are altered. This damage is usually represented by a decrease in the stiffness of the structure locally. This damage in an element is modeled with a damage parameter D which represents a reduction in flexural rigidity of the element and is defined as

$$D = \frac{(EI)_u - (EI)_d}{(EI)_u} \times 100 \tag{11}$$

where subscripts u,d represent the undamaged and damaged states of the beam elements, respectively.

For numerical studies, the damage is varied from 0% to 50% and the location of damage is also varied along the length of the beam.

4 Results and Discussion

The beam analyzed here has the following properties: $E = 200\ GPa$, $I = 2000\ mm^4$, $A = 240\ mm$, $\rho = 7800\ kg/m^3$ and $L = 1\ m$. The natural frequencies and mode shapes are computed using the methodology described in the previous section. Fig. 2 shows the first five mode shapes for the beam considered here. The finite element analysis of the beam is done by dividing it into 20 finite elements of equal length and these results are validated with the exact solutions for a uniform beam.

4.1 Spatial Fourier Analysis of Undamaged Beam

The undamaged beam is analyzed using the analytical and FEM methods and the Fourier coefficients are obtained for the first five modes. The non-zero Fourier coefficients are presented in Tab. 1 through Tab. 5, respectively. Here it is observed that the analytical or exact solution matches exactly with the FEM solution up to

the 5^{th} decimal. Hence the mode shapes can be represented by the finite element model with good accuracy. It is found that for the 1^{st}, 3^{rd} and 5^{th} modes, all b_j, $(j = 1,2,3,...)$ are zeros and non-zero coefficients for each mode are given in Tab. 1, Tab. 3 and Tab. 5 respectively. For the 2^{nd} mode, it is observed that all a_i, b_j ,$(i = 1,2,3,..., j = 2,3,...)$ are zeros which leaves only a non-zero b_1 which is equal to unity and is shown in Tab. 2. For the 4^{th} mode, all a_i, b_j are zero except for b_2 which is unity (Tab. 4) . Further modes can be used to draw some general conclusions. The trend in all odd number modes is same with all b_j,$(j = 1,2,3,...)$ being zero. For the even number modes, all a_i,b_j are zero except for the $b_{\frac{n}{2}}$ coefficient for mode n. For the 2^{nd} mode, b_1 is unity. For the 4^{th} mode, b_2 is unity. For the 6^{th} mode, b_3 is unity and so on. Physically, this shows that the even modes are pure sine components as can also be seen from Fig. 2. The odd modes consists of a constant part and cosine components. It is also observed that the steady and fundamental harmonics are dominant and other harmonics show a rapid decrease for higher harmonics.

Table 1: Non-zero Fourier coefficients for first mode of an undamaged simply supported beam

Coefficient	Analytical value	Normalized value	FE value
a_0	0.6366	1.00000	0.6366
a_1	-0.4245	-0.66682	-0.4245
a_2	-0.08502	-0.13335	-0.08502
a_3	-0.03651	-0.05735	-0.03651
a_4	-0.02035	-0.03196	-0.02035
a_5	-0.01301	-0.02043	-0.01301
a_6	-0.00906	-0.01423	-0.00906
a_7	-0.00669	-0.01052	-0.00669
a_8	-0.00517	-0.00081	-0.00517
a_9	-0.00414	-0.00065	-0.00414
a_{10}	-0.00326	-0.00051	-0.00326

Table 2: Non-zero Fourier coefficients for second mode of an undamaged simply supported beam

Coefficient	Analytical value	Normalized value	FE value
b_1	1.00000	1.00000	1.00000

Table 3: Non-zero Fourier coefficients for third mode of an undamaged simply supported beam

Coefficient	Analytical value	Normalized value	FE value
a_0	0.21200	0.27766	0.21200
a_1	0.76350	1.00000	0.76350
a_2	-0.54600	-0.71512	-0.54600
a_3	-0.14190	-0.18585	-0.14190
a_4	-0.06987	-0.09151	-0.06987
a_5	-0.04242	-0.05555	-0.04242
a_6	-0.02877	-0.03768	-0.02877
a_7	-0.02093	-0.02741	-0.02093
a_8	-0.01602	-0.02098	-0.01602
a_9	-0.01274	-0.01668	-0.01274
a_{10}	-0.00999	-0.01308	-0.00999

Table 4: Non-zero Fourier coefficients for fourth mode of an undamaged simply supported beam

Coefficient	Analytical value	Normalized value	FE value
b_2	1.00000	1.00000	1.00000

Table 5: Non-zero Fourier coefficients for fifth mode of an undamaged simply supported beam

Coefficient	Analytical value	Normalized value	FE value
a_0	0.12690	-0.17966	0.12690
a_1	0.30230	-0.42800	0.30230
a_2	-0.70630	1.00000	-0.70630
a_3	-0.57920	0.82004	-0.57920
a_4	-0.16390	0.23205	-0.16390
a_5	-0.08560	0.12119	-0.08560
a_6	-0.05427	0.07683	-0.05427
a_7	-0.03807	0.05390	-0.03807
a_8	-0.02849	0.04033	-0.02849
a_9	-0.02234	0.03162	-0.02234
a_{10}	-0.01734	0.02455	-0.01734

4.2 Spatial Fourier Analysis of Damaged Beam

In this section the effect of damage on the Fourier coefficients of mode shapes is discussed. The developed finite element model is used to find out the Fourier coefficient for first three modes and at various damage levels ranging from 0% to 50% and for the elements $1, 5$ and 10 (see Fig. 1). The variation in the constant and first five harmonic Fourier coefficients is shown in Fig. 3 through Fig. 8. In these figures, a_{35} represents the a_3 Fourier coefficient for damage in element 5, as an example. These graphs show that the Fourier coefficients are sensitive to damage. There is an increase in the Fourier coefficients as compared to the undamaged mode as the damage increases from 0 *to* 50 percentage. Also, it can be observed that the coefficients b_j, $(j = 1,2,3,...)$ for 1^{st} and 3^{rd} modes and a_i, b_j, $(i = 1,2,3,...)$, $(j = 2,3,...)$ for the 2^{nd} mode now possess *non-zero values due to the presence of damage*. These values increase monotonically with damage. Hence, the occurrence of above mentioned coefficients in the modes denotes the presence of damage.

Further, the b_j, $(j = 1,2,3,...)$ coefficients in 1^{st}, 3^{rd} modes and a_i, $(i = 1,2,3,...)$ coefficients in 2^{nd} mode are *antisymmetric with respect to damage location*. These antisymmetric coefficients are useful for detecting damage in the symmetric locations of the beam like 5^{th} and 16^{th} elements. In these locations, the symmetric coefficients show same value. In general, for all odd number of modes a_i are symmetric and b_j are antisymmetric and for all even number of modes b_j are symmetric and a_i are antisymmetric. Therefore, it is observed that for unique representation of the damage at any location at least one set of symmetric and antisymmetric coefficients are needed.

The spatial Fourier coefficients can therefore serve as damage indicators for beams which are simply supported at both ends.

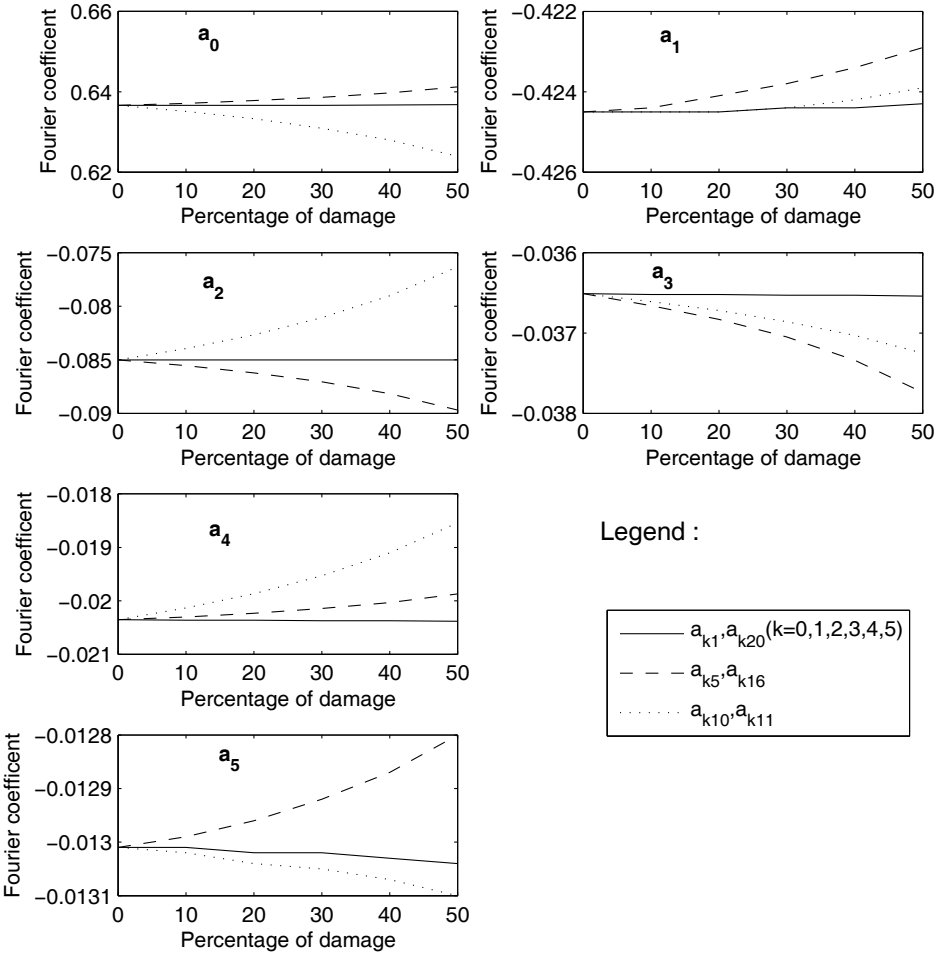

Figure 3: Variation of Constant and Cosine Fourier coefficients for 1^{st} mode in different elements

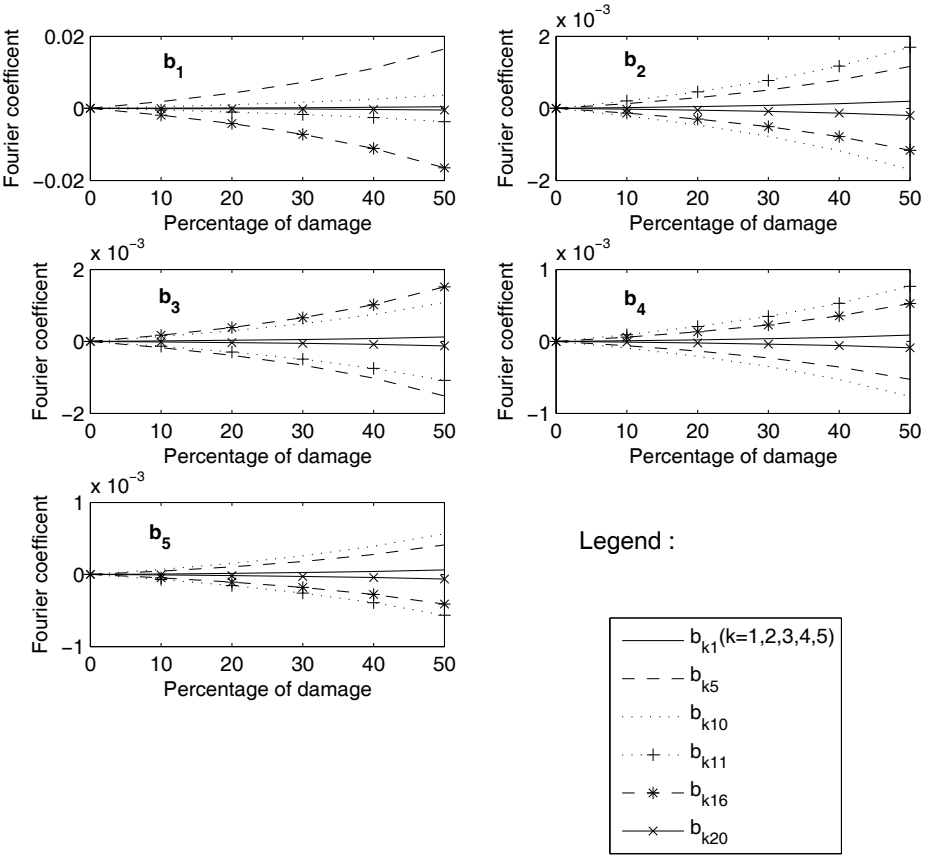

Figure 4: Variation of Sine Fourier coefficients for 1^{st} mode in different elements

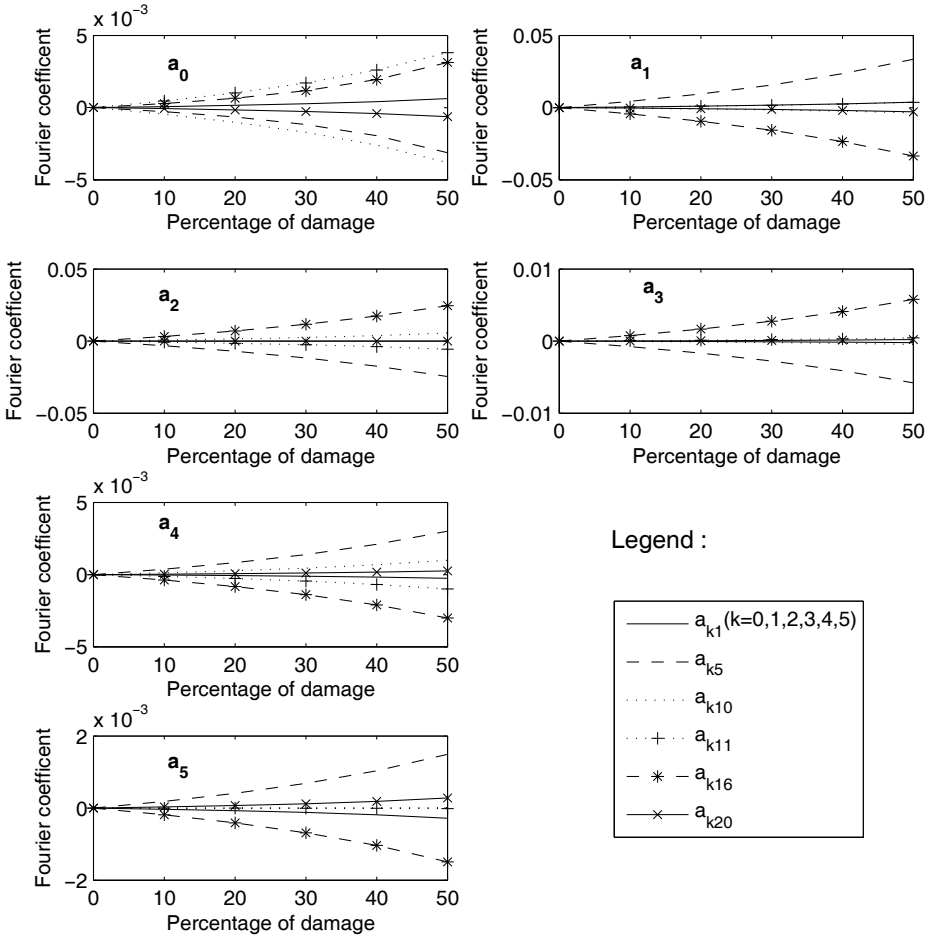

Figure 5: Variation of Constant and Cosine Fourier coefficients for 2^{nd} mode in different elements

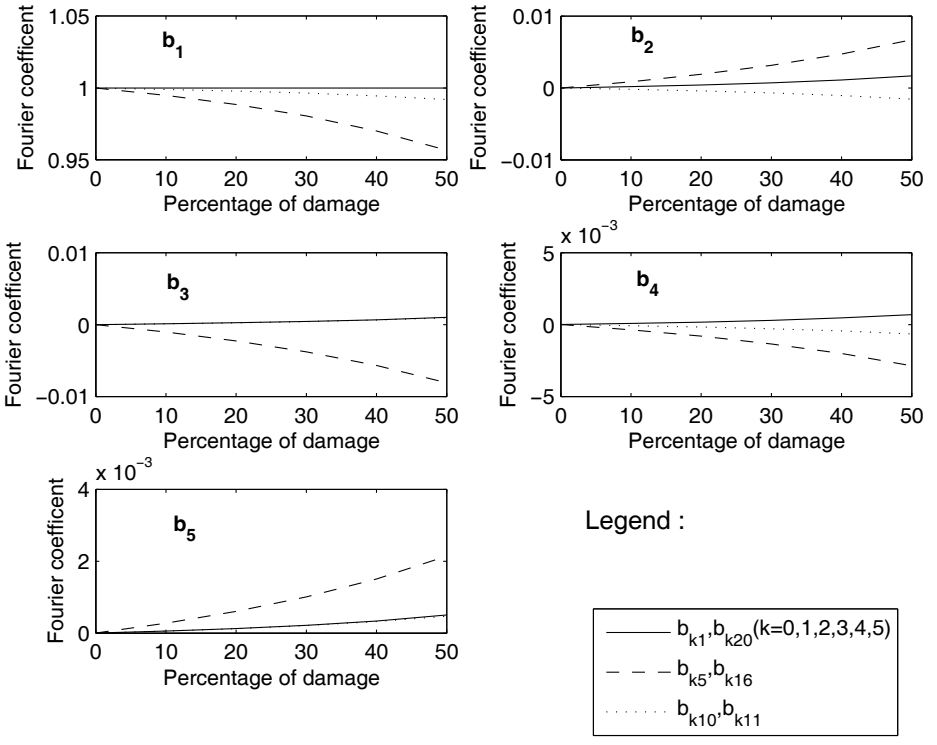

Figure 6: Variation of Sine Fourier coefficients for 2^{nd} mode in different elements

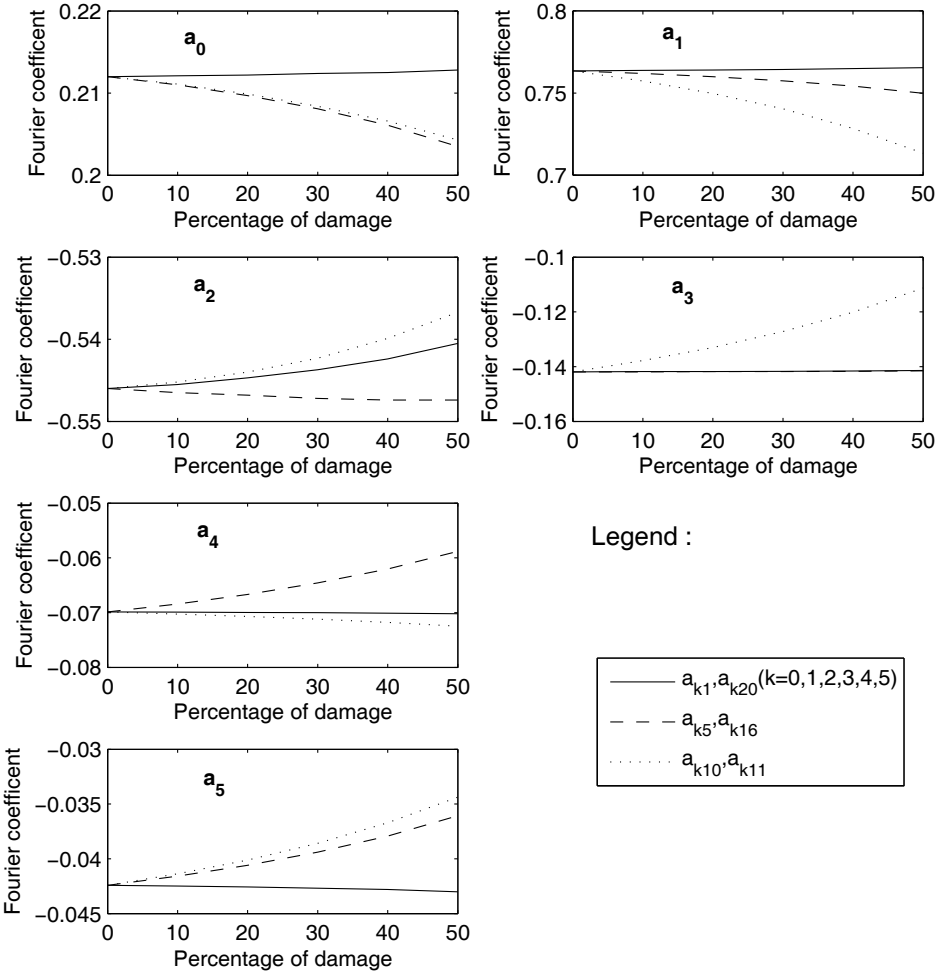

Figure 7: Variation of Constant and Cosine Fourier coefficients for 3^{rd} mode in different elements

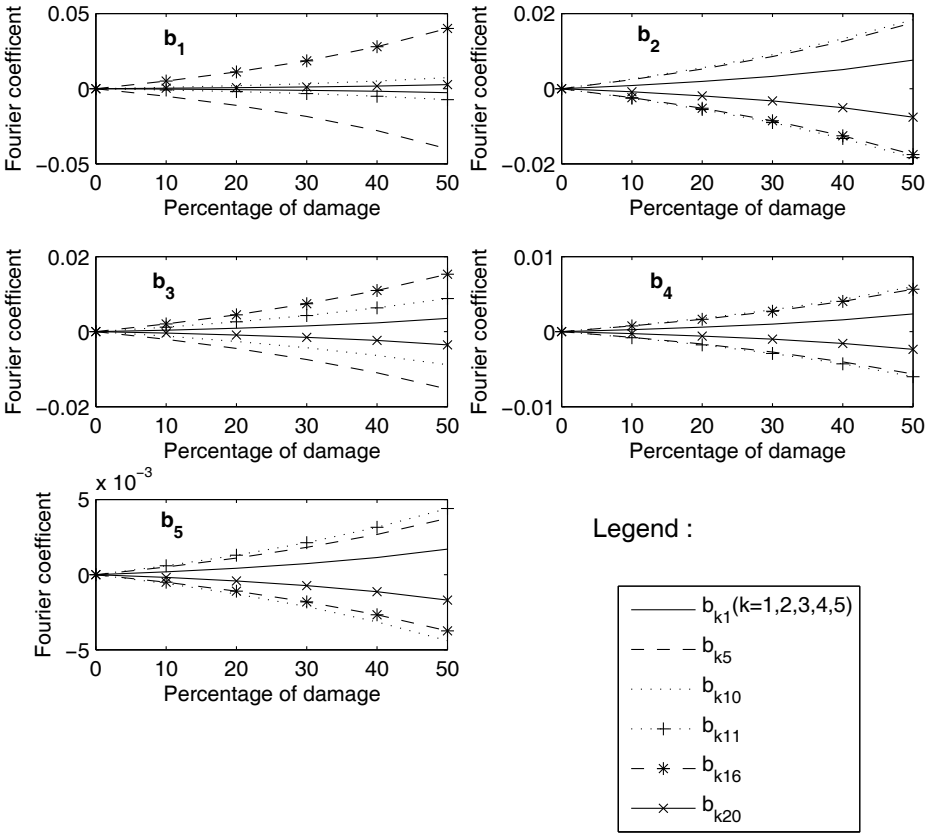

Figure 8: Variation of Sine Fourier coefficients for 3^{rd} mode in different elements

4.2.1 Noisy Data

The output of mathematical model and that of the test always differ because of the experimental noise and measurement errors. Use of modern instruments reduces the measurement errors but they can never be eliminated. To simulate this noise we shall assume that 1% noise is present in the mode shape. The noisy mode shape vector is given by the Eq. 12

$$\Phi_{noisy}(i) = \Phi_{ideal}(i) + \alpha * rand() \tag{12}$$

Here α is the noise level which is 0.01 and the function $rand()$ generates random numbers varying from $-1\,to+1$. Here Φ is the vector containing the mode shapes. For analyzing the effect of damage on mode shapes in presence of noise, 20 noisy sample are created using the Eq. 12. Fig. 9 gives a sample ideal and noisy mode shape for the first three modes. The corresponding Fourier coefficients are plotted for the first, fifth and tenth elements (Fig. 10 to Fig. 27).

From these figures, the Fourier coefficients which are least affected by the presence of noise and sensitive to damage size and location are identified.

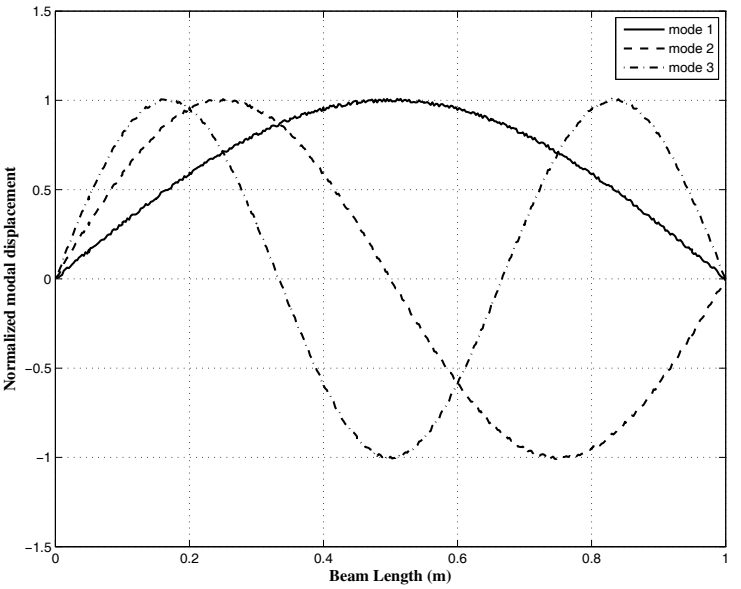

Figure 9: First Three Noisy modes of an undamaged beam

Fig. 10 and 11 show the Fourier coefficients for the 1^{st} mode with increasing damage levels in the 1^{st} element. It can be seen that the noise leads to considerable scatter in the coefficients. Fig. 12 and 13 show the Fourier coefficients for the noisy 1^{st} mode for the 5^{th} element. Here we can see the coefficients a_2 in Fig. 12 and b_1 in Fig. 13 show relatively low effect of noise and also show considerable change due to damage level. Thus, a_2 and b_1 for the 1^{st} mode can serve as good indicators of damage in the 5^{th} element. Tab. 6 lists the selected Fourier coefficients for different elements and different modes. Fig. 14 and 15 show the Fourier coefficients for the noisy 1^{st} mode for the 10^{th} element. Here we see that a_0 and a_2 are good damage indicators showing low scatter and considerable monotonic variation with damage.

We now study the 2^{nd} mode coefficients. Fig. 16 and 17 show the Fourier coefficients for the noisy 2^{nd} mode with damage in the first element. We see considerable scatter in all the Fourier coefficients here. Fig. 18 and 19 show the Fourier coefficients for the noisy 2^{nd} mode with damage in the 5^{th} element. From Fig. 18, it is clear that a_1 and a_2 show low scatter and good monotonic change with damage size. From Fig. 19, we can see that b_1 is a good damage indicator for the 5^{th} element. Fig. 20 and 21 give the Fourier coefficients for the noisy 2^{nd} mode with damage in the 10^{th} element. Here we choose a_2 and b_1 are the coefficients with low scatter and considerable change due to damage size.

Finally, we study the 3^{rd} mode coefficients. Fig. 22 and 23 show the Fourier coefficients for the noisy 3^{rd} mode with damage in the 1^{st} element. Here, a_2 and b_2 show low scatter and high sensitivity to damage size. Fig. 24 and 25 show the Fourier coefficients for the noisy 3^{rd} mode with damage in the 5^{th} element. Here, a_0, a_1, a_4, b_1 and b_2 show low scatter and considerable change with damage size. Fig. 26 and 27 show the Fourier coefficients for the noisy 3^{rd} mode with damage in the 10^{th} element. Here, a_1, a_3, b_2 show very low sensitivity to noise and a significant change due to size of damage.

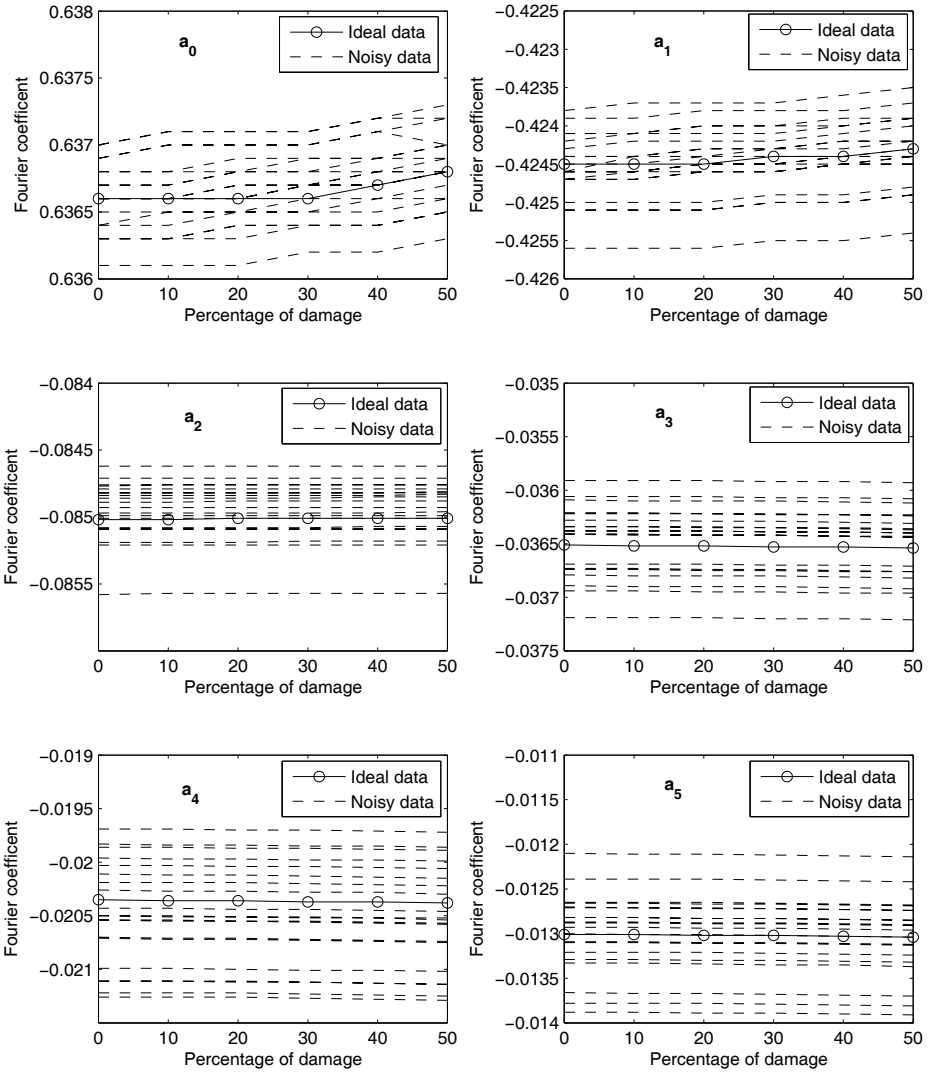

Figure 10: Variation of Constant and Cosine Fourier coefficients for Noisy 1^{st} mode in 1^{st} element (20 noisy samples)

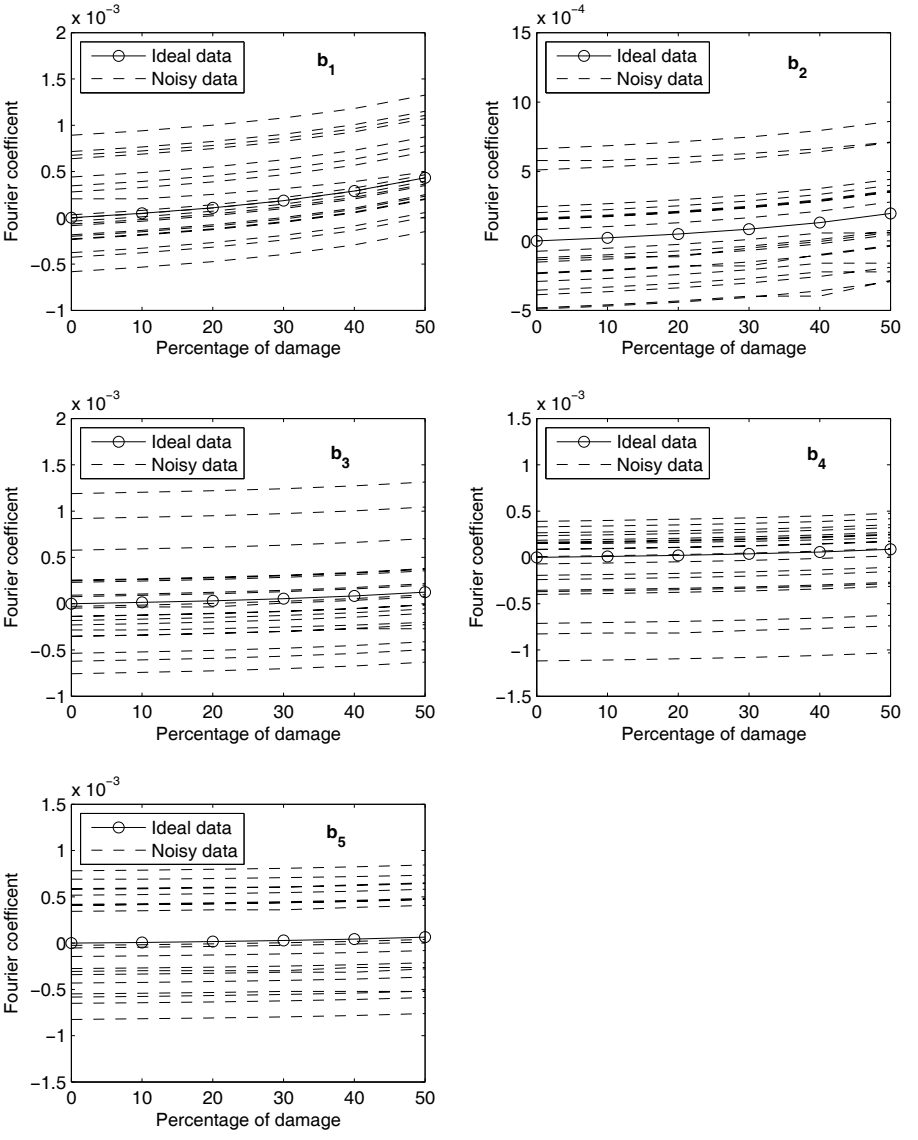

Figure 11: Variation of Sine Fourier coefficients for Noisy 1^{st} mode in 1^{st} element (20 noisy samples)

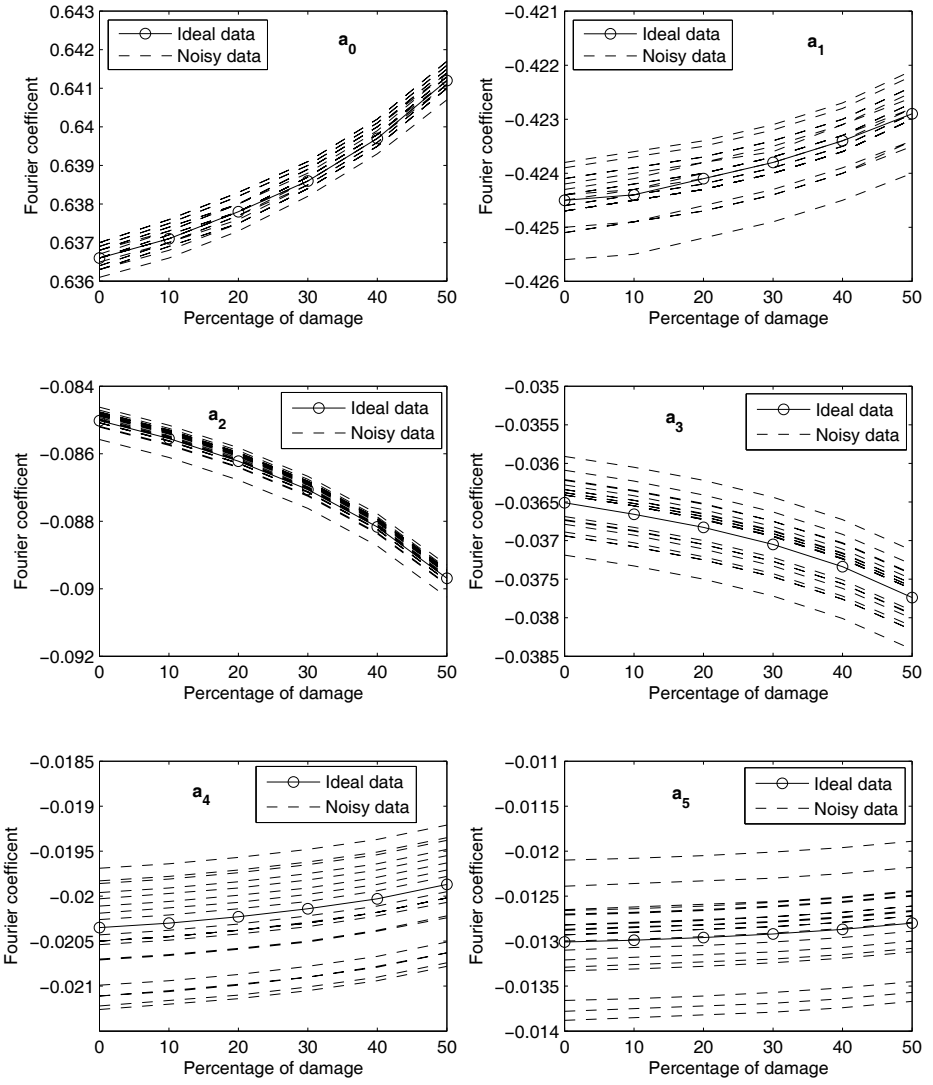

Figure 12: Variation of Constant and Cosine Fourier coefficients for Noisy 1^{st} mode in 5^{th} element (20 noisy samples)

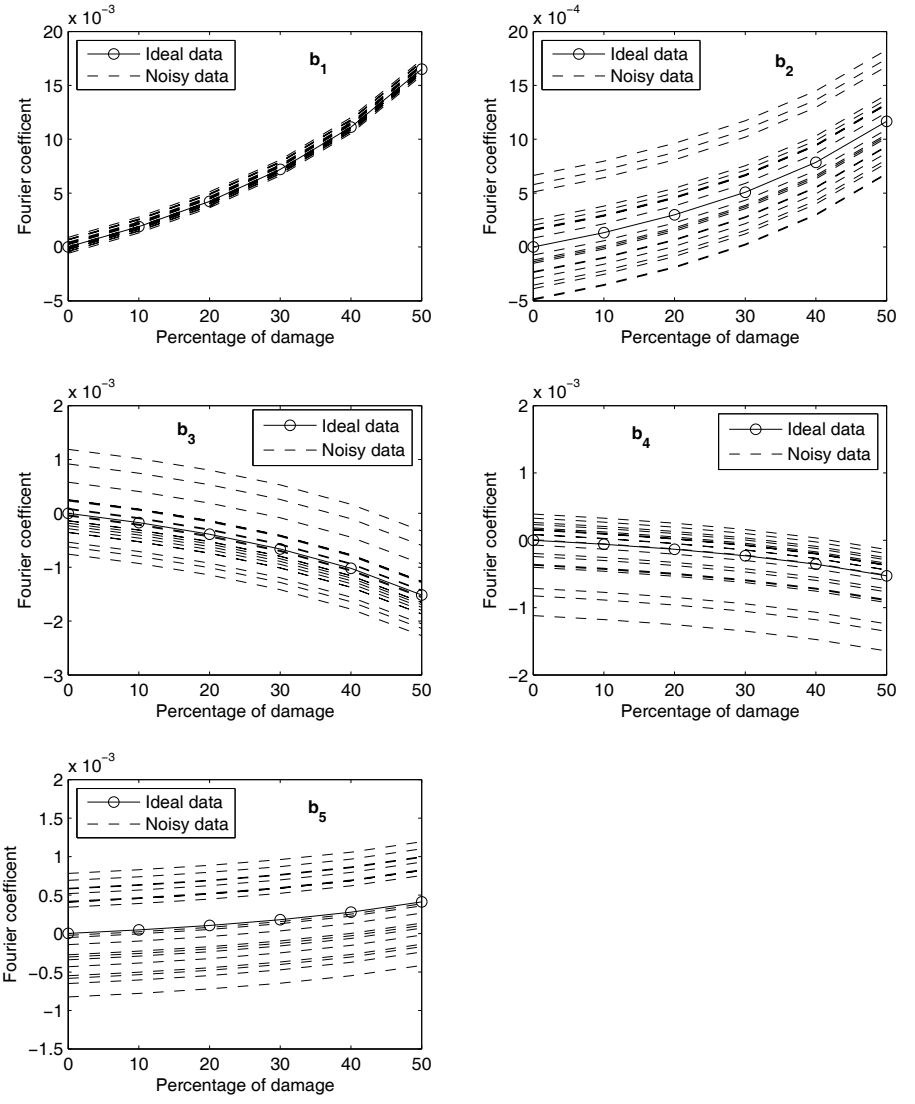

Figure 13: Variation of Sine Fourier coefficients for Noisy 1^{st} mode in 5^{th} element (20 noisy samples)

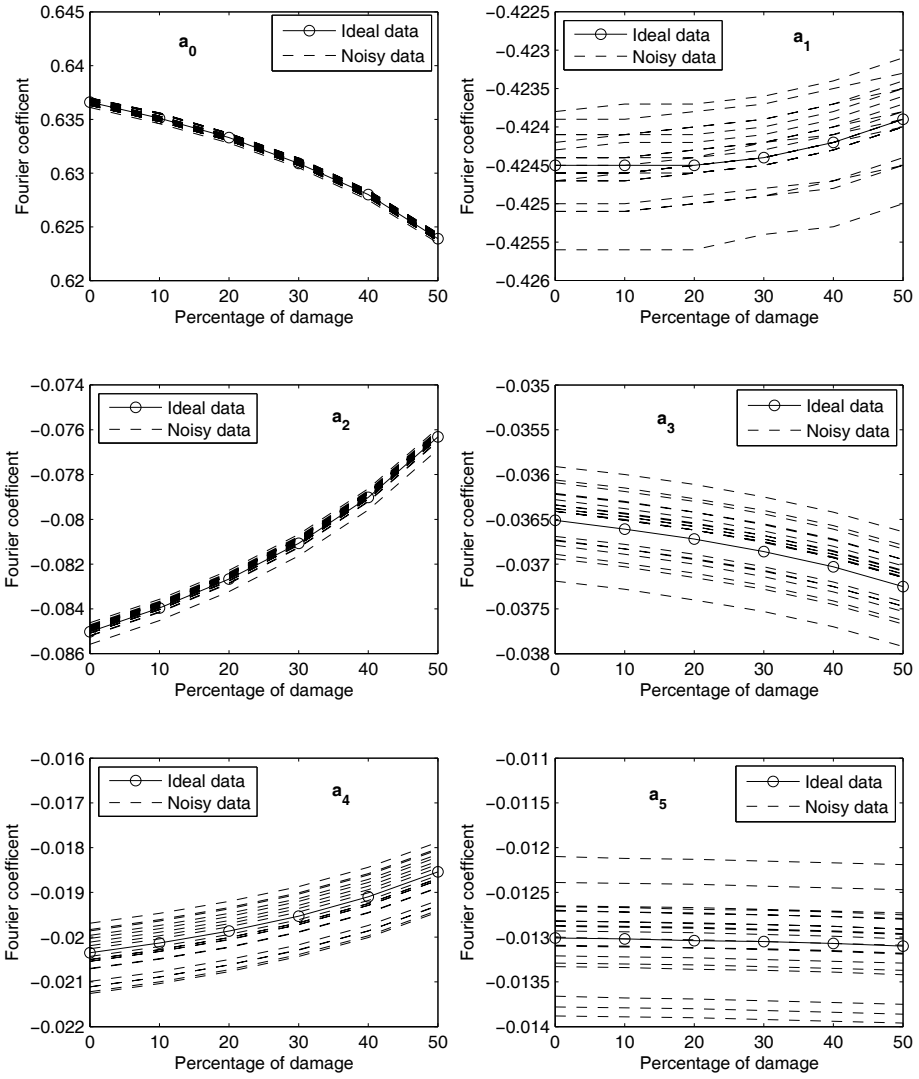

Figure 14: Variation of Constant and Cosine Fourier coefficients for Noisy 1^{st} mode in 10^{th} element (20 noisy samples)

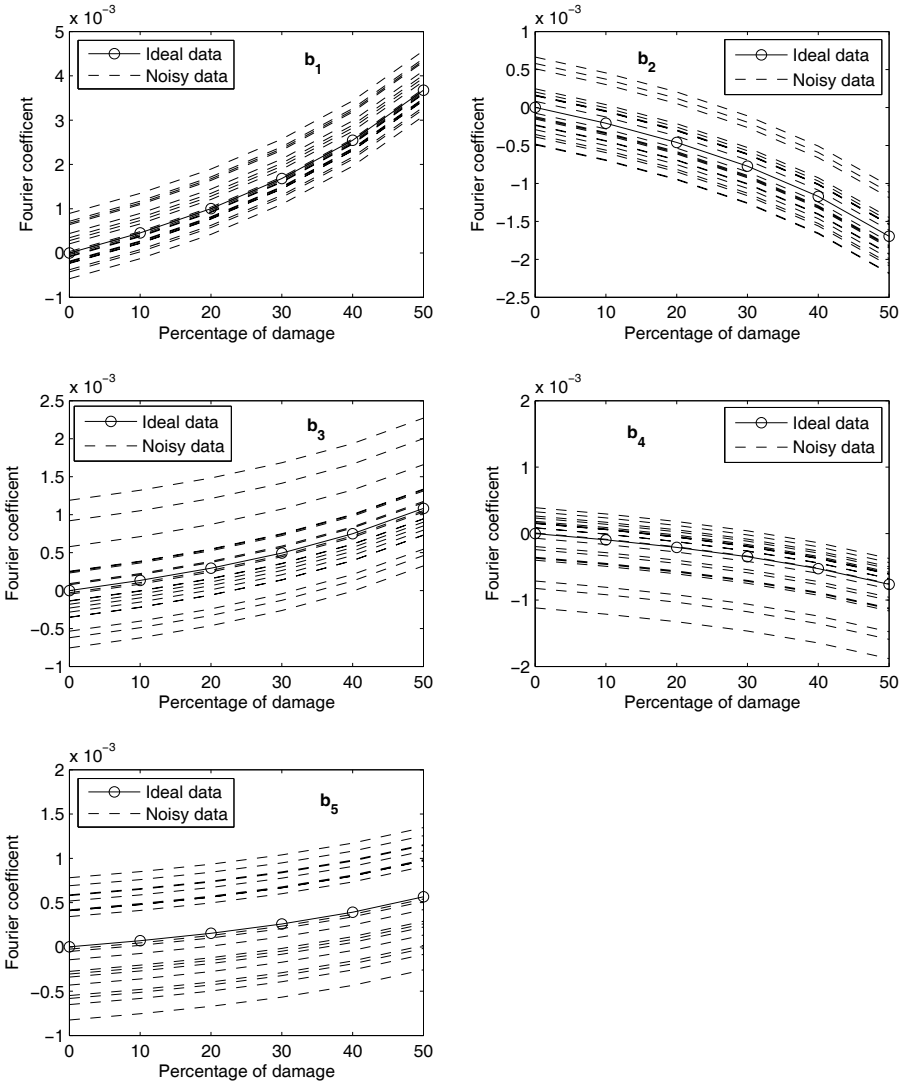

Figure 15: Variation of Sine Fourier coefficients for Noisy 1^{st} mode in 10^{th} element (20 noisy samples)

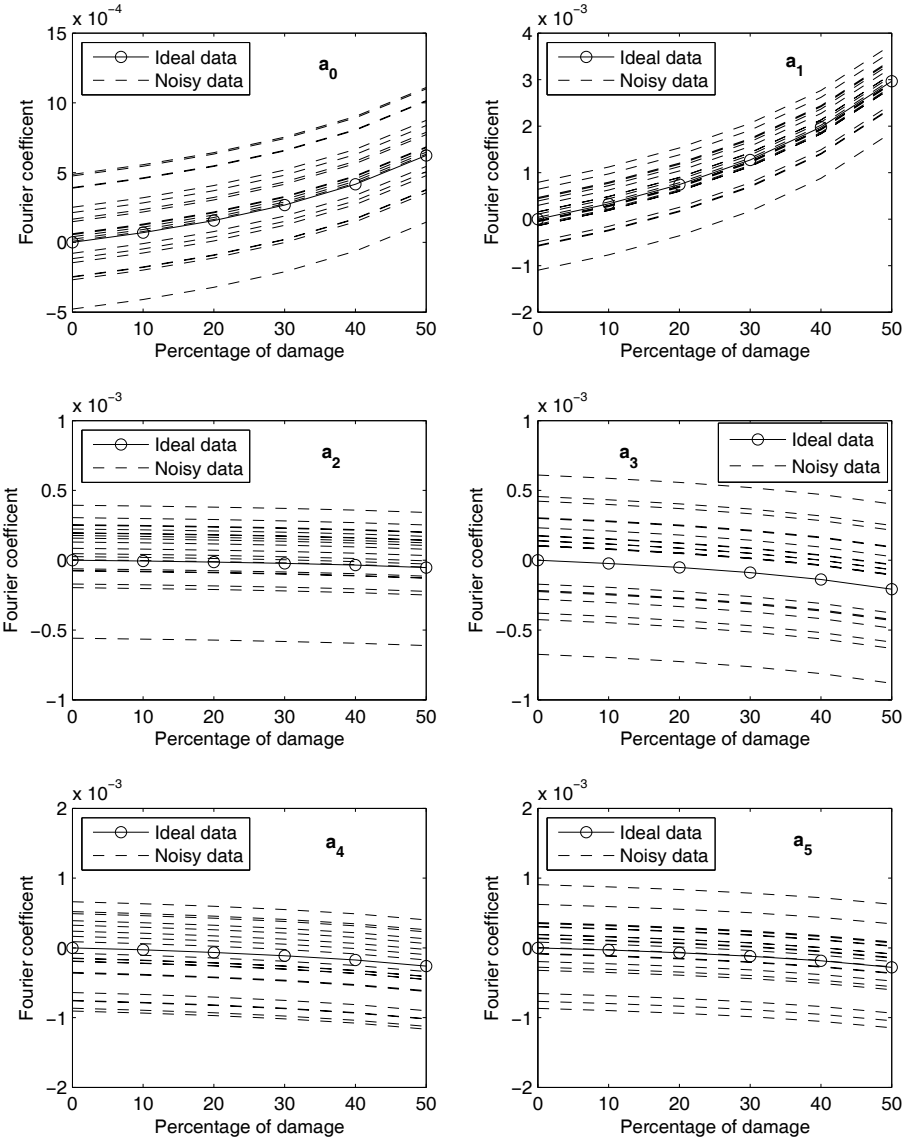

Figure 16: Variation of Constant and Cosine Fourier coefficients for Noisy 2^{nd} mode in 1^{st} element (20 noisy samples)

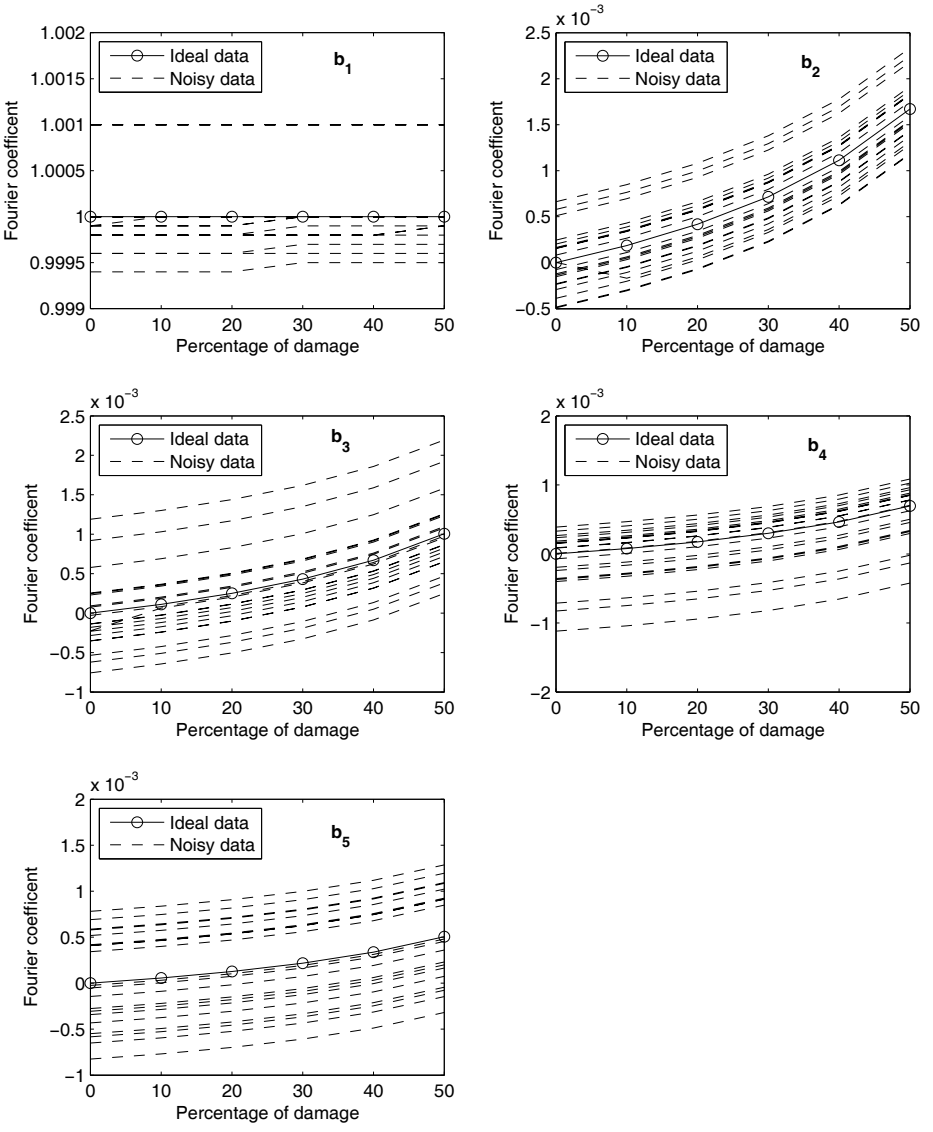

Figure 17: Variation of Sine Fourier coefficients for Noisy 2^{nd} mode in 1^{st} element (20 noisy samples)

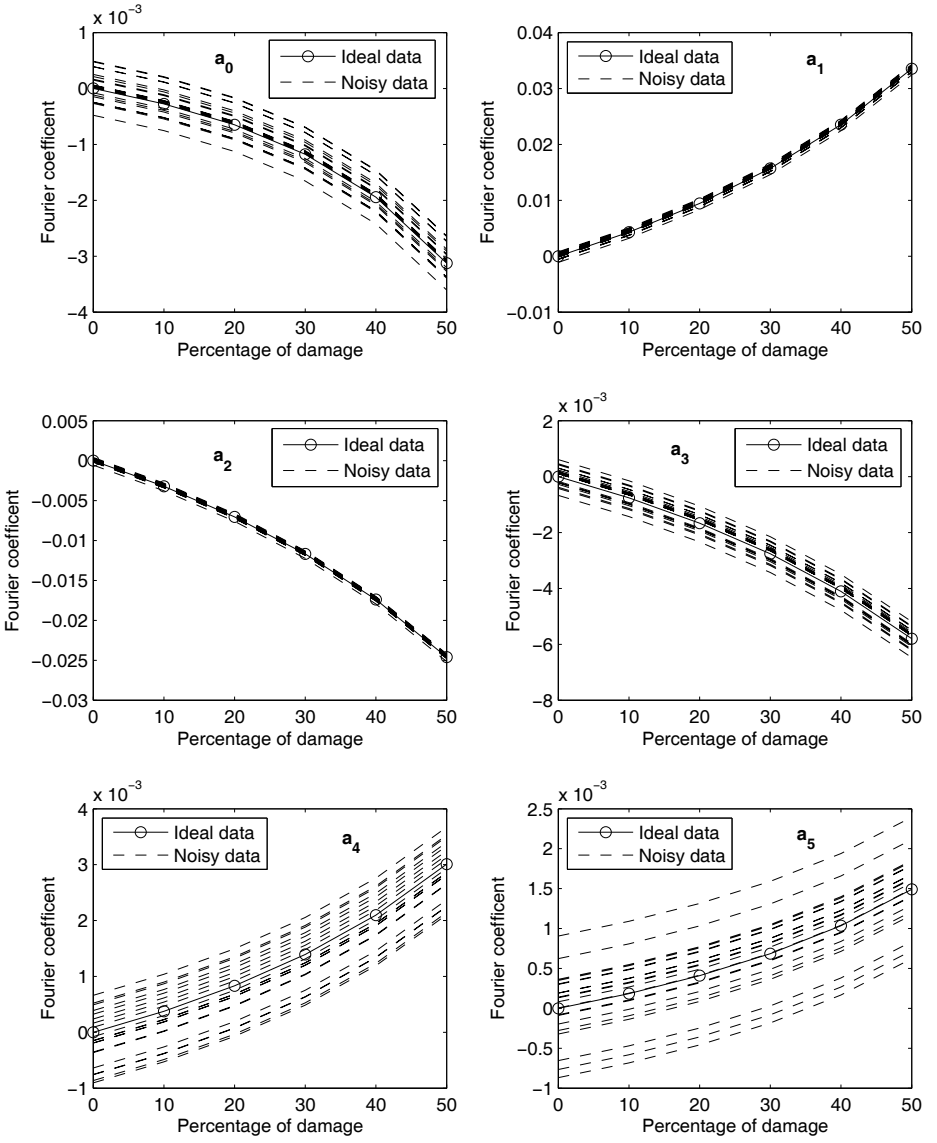

Figure 18: Variation of Constant and Cosine Fourier coefficients for Noisy 2^{nd} mode in 5^{th} element (20 noisy samples)

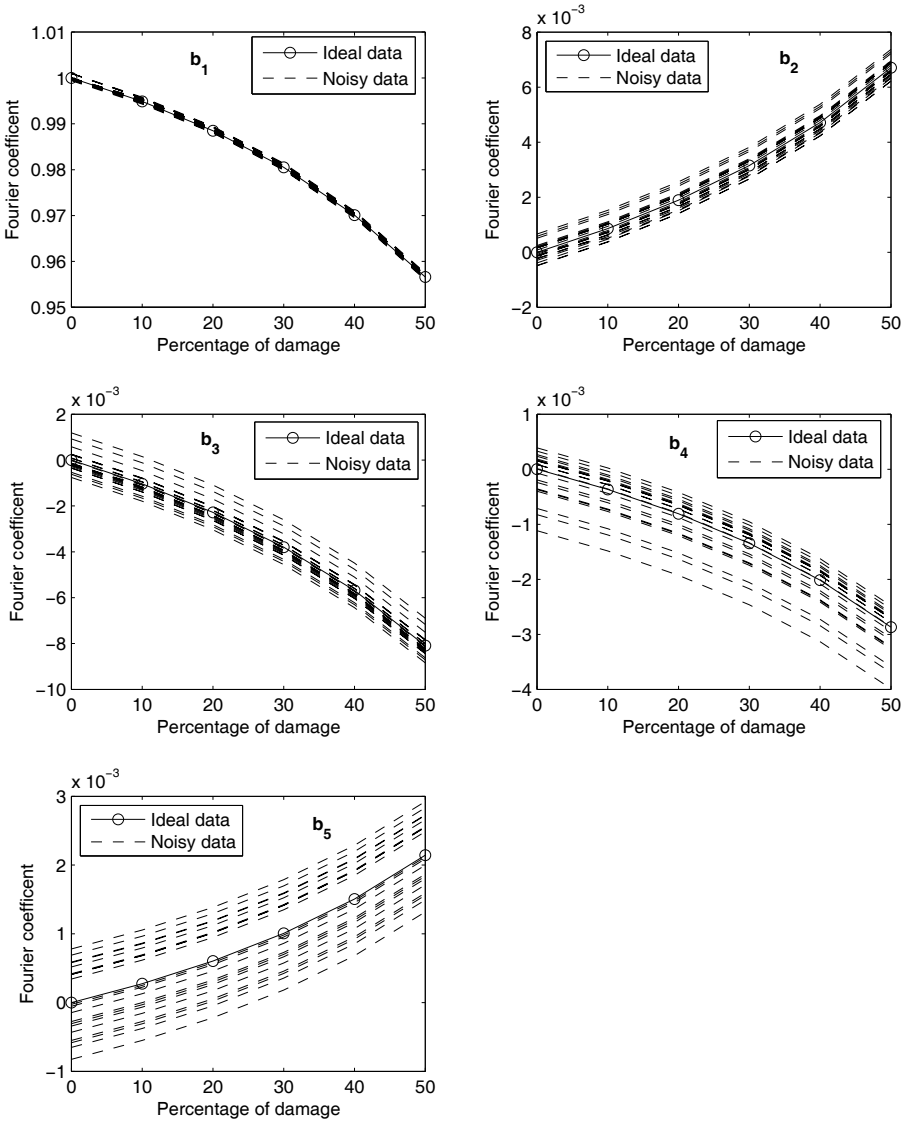

Figure 19: Variation of Sine Fourier coefficients for Noisy 2^{nd} mode in 5^{th} element (20 noisy samples)

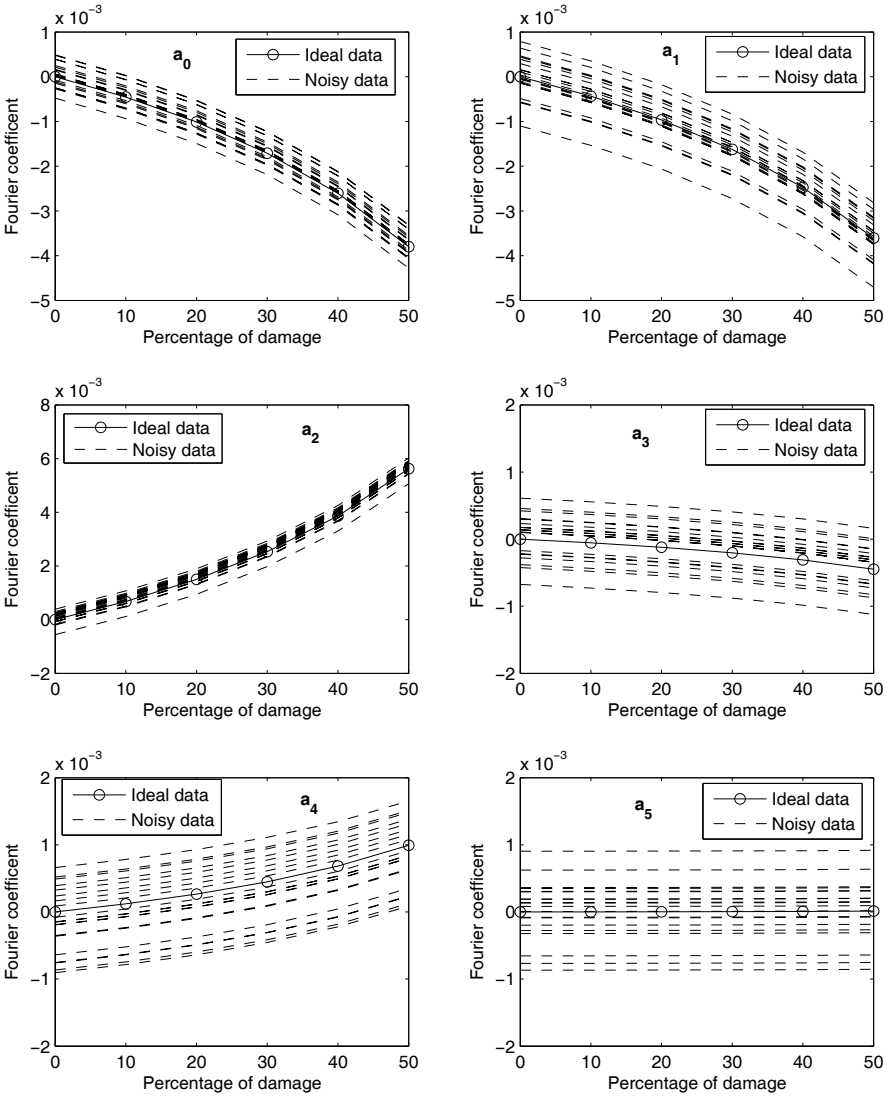

Figure 20: Variation of Constant and Cosine Fourier coefficients for Noisy 2^{nd} mode in 10^{th} element (20 noisy samples)

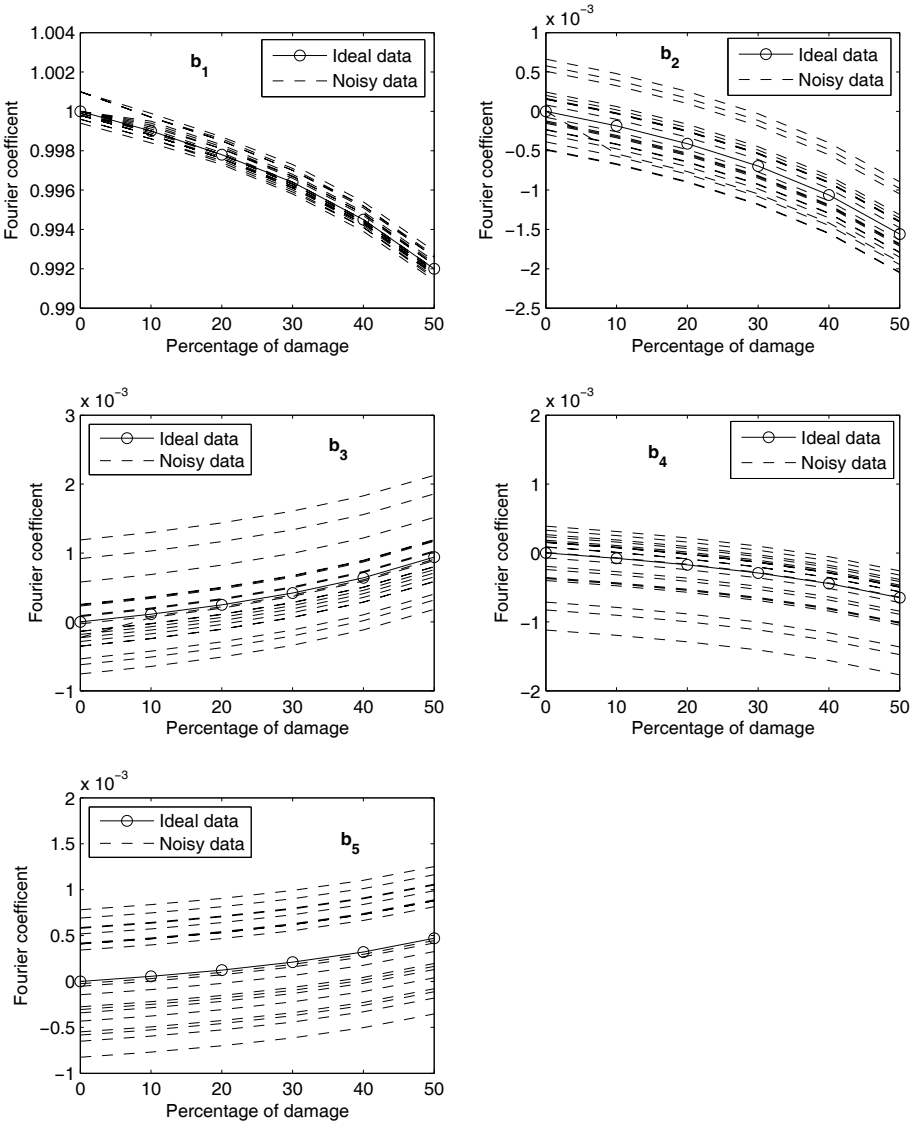

Figure 21: Variation of Sine Fourier coefficients for Noisy 2^{nd} mode in 10^{th} element (20 noisy samples)

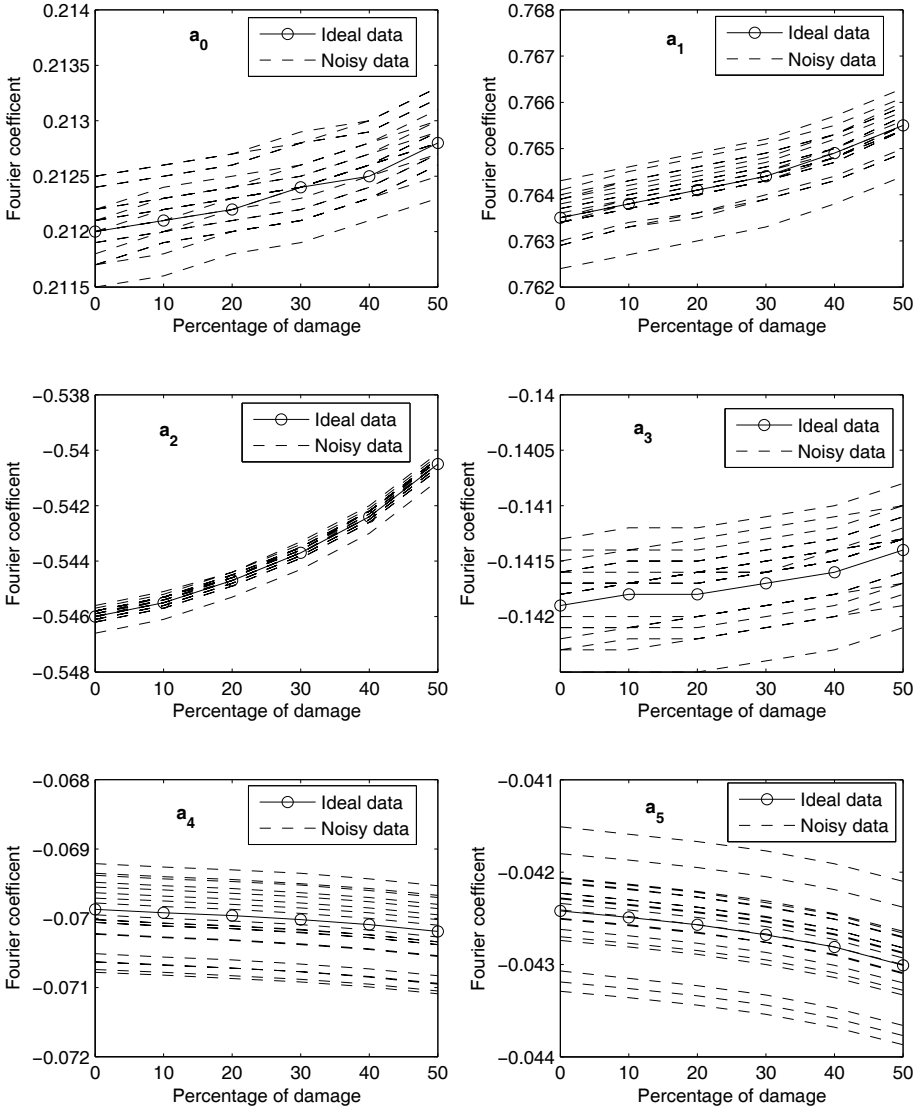

Figure 22: Variation of Constant and Cosine Fourier coefficients for Noisy 3^{rd} mode in 1^{st} element (20 noisy samples)

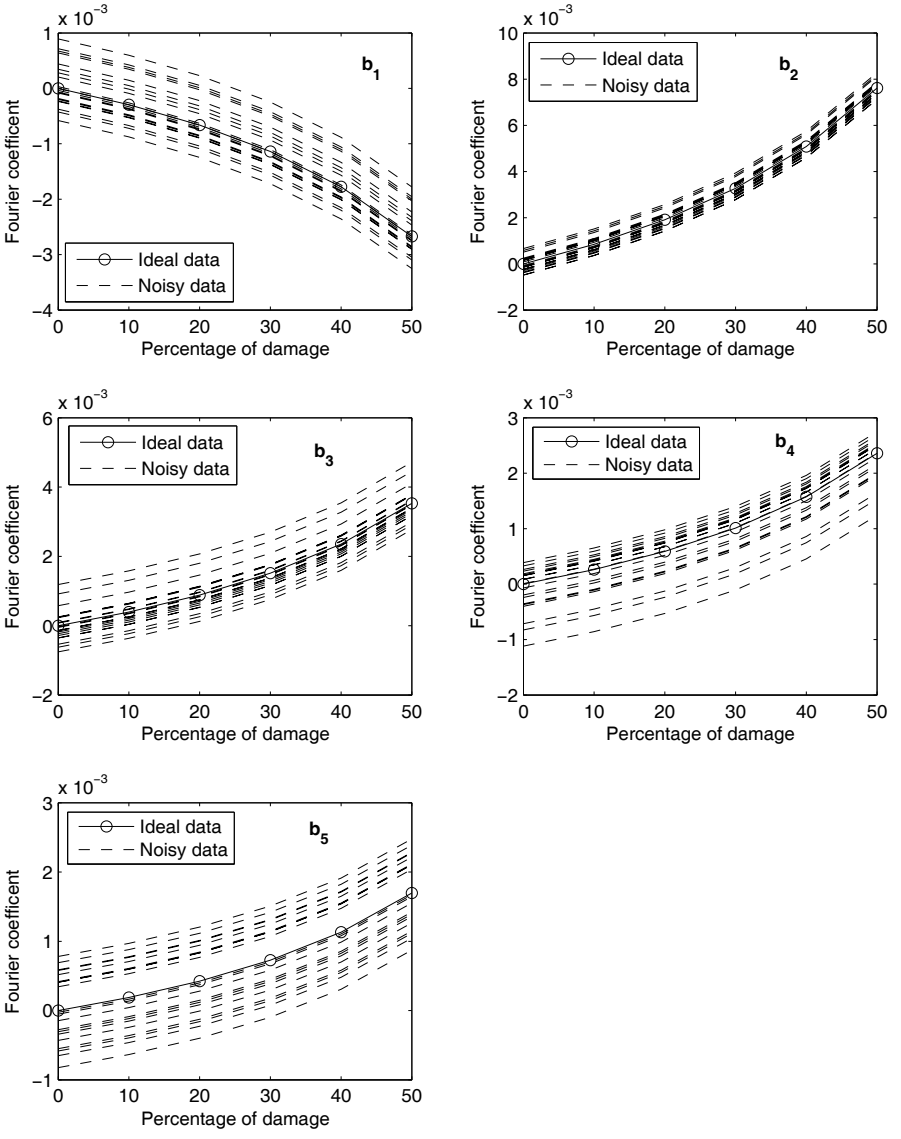

Figure 23: Variation of Sine Fourier coefficients for Noisy 3^{rd} mode in 1^{st} element (20 noisy samples)

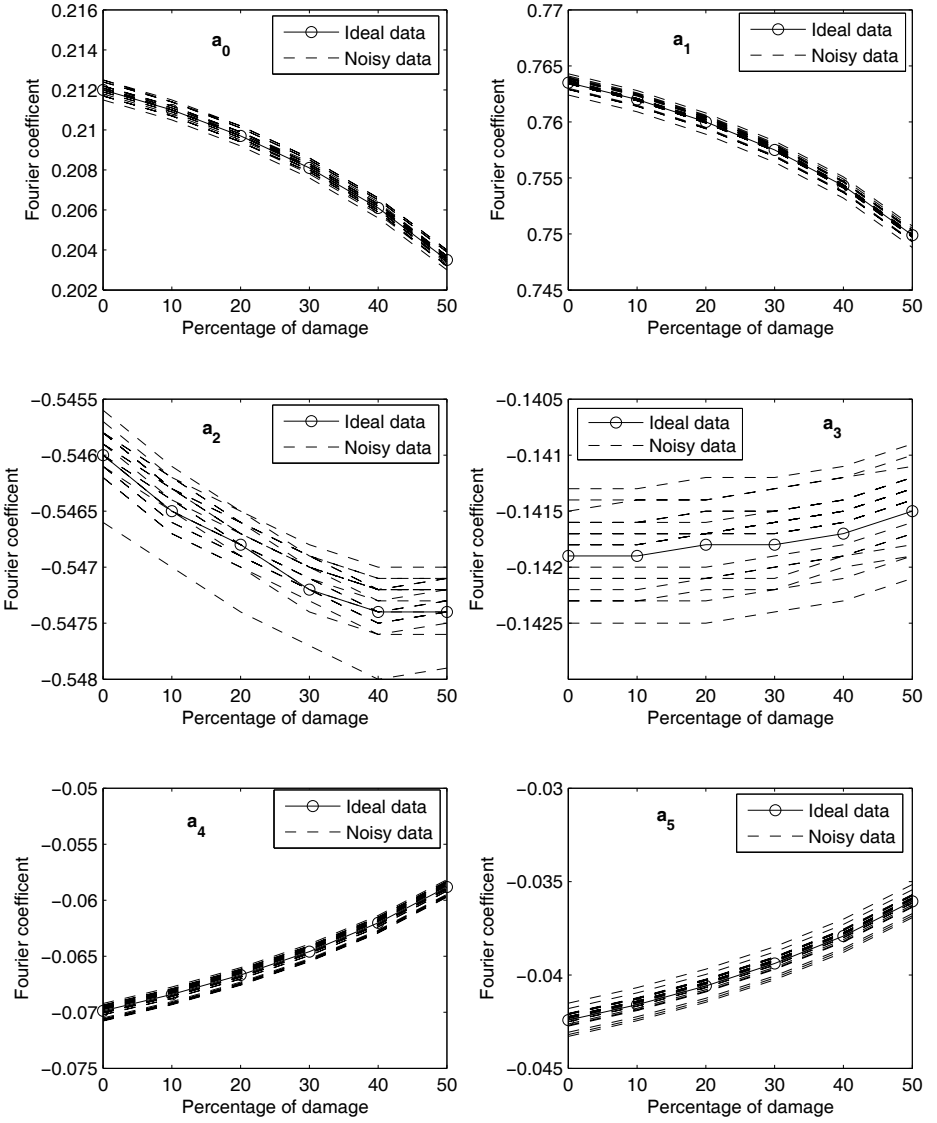

Figure 24: Variation of Constant and Cosine Fourier coefficients for Noisy 3^{rd} mode in 5^{th} element (20 noisy samples)

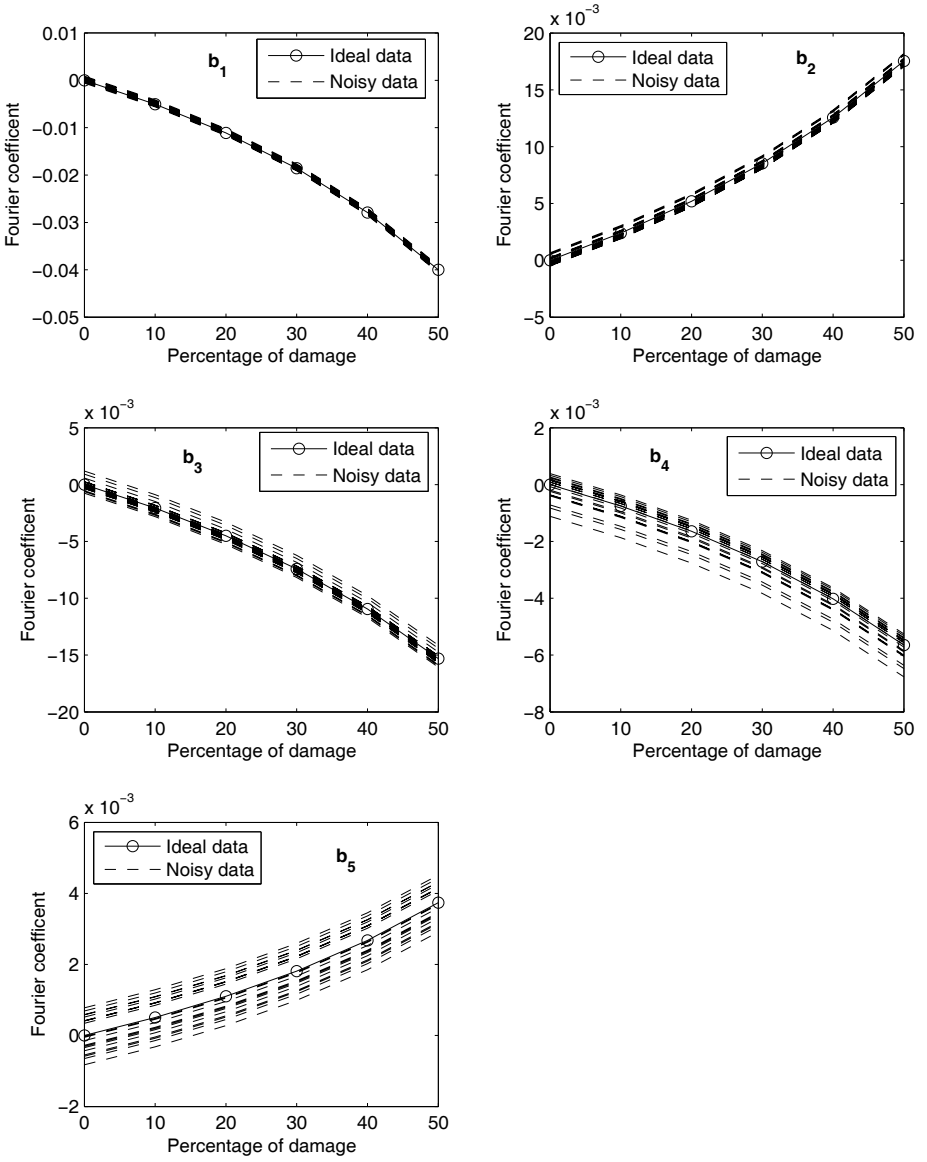

Figure 25: Variation of Sine Fourier coefficients for Noisy 3^{rd} mode in 5^{th} element (20 noisy samples)

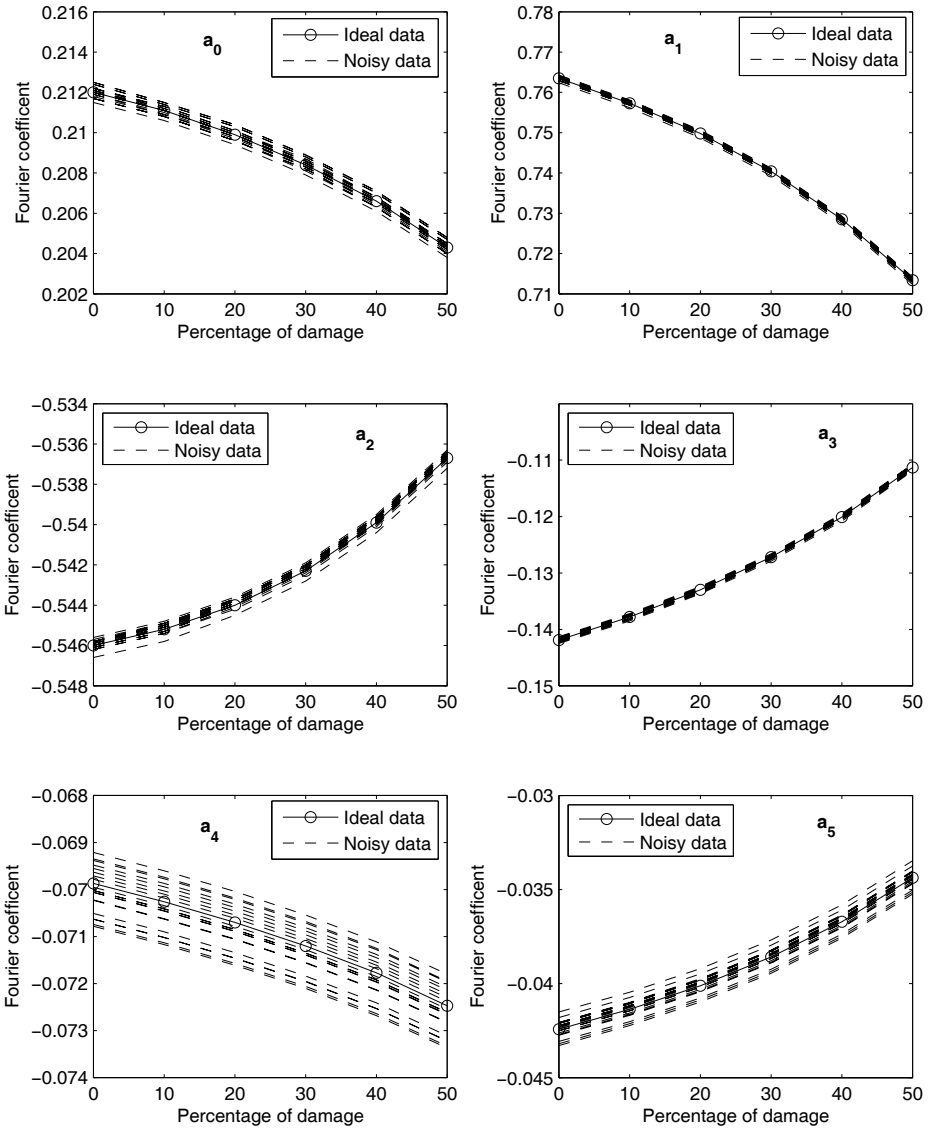

Figure 26: Variation of Constant and Cosine Fourier coefficients for Noisy 3^{rd} mode in 10^{th} element (20 noisy samples)

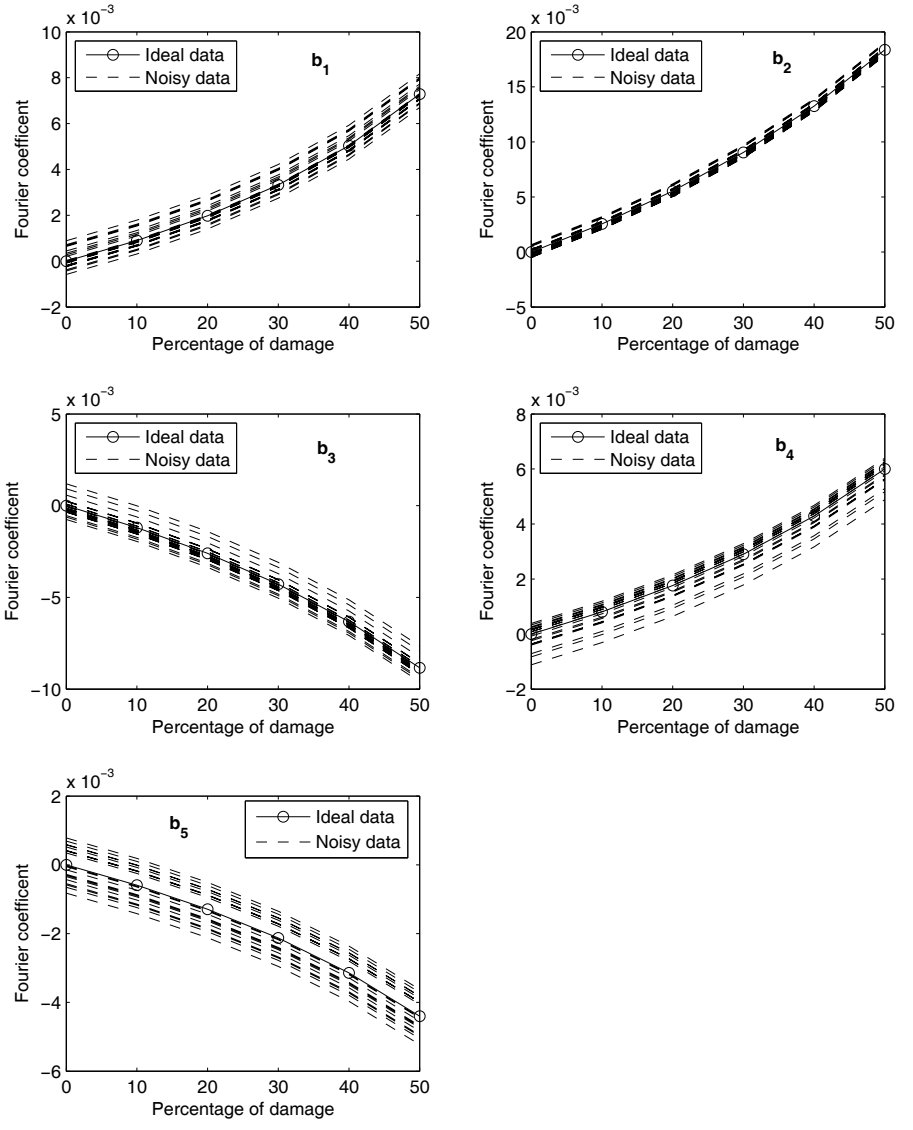

Figure 27: Variation of Sine Fourier coefficients for Noisy 3^{rd} mode in 10^{th} element (20 noisy samples)

Table 6: Selected Fourier coefficients which indicate damage in presence of noise

Damage location	Mode 1	Mode 2	Mode 3
1			a_2, b_2
5	a_2, b_1	a_1, a_2, b_1	a_0, a_1, a_4, b_1, b_2
10	a_0, a_2	a_2, b_1	a_1, a_3, b_2
11	a_0, a_2	$-a_2, b_1$	$a_1, a_3, -b_2$
16	$a_2, -b_1$	$-a_1, -a_2, b_1$	$a_0, a_1, a_4, -b_1, -b_2$
20			$a_2, -b_2$

Note that damage in element 20 also causes changes in coefficient a_2. Now, for representing the damage in element 20, we use the antisymmetric coefficient b_2 which is represented as $-b_2$ in the Tab. 6. The negative sign points to the opposite pattern of variation relative to the element 1. So, for every damage size and location pair there is a unique set of sensitive Fourier coefficients which can be used as unique and effective damage indicators for that particular damage location and size.

The numerical results of this paper show that spatial Fourier coefficients amplify the effect of damage in mode shapes and some of the coefficients are robust to the presence of noise and grow significantly and monotonically with damage size. They constitute an attractive damage indicator for beams simply supported at both ends.

5 Conclusions

Spatial Fourier analysis of mode shapes for a beam simply supported at both ends is done. A finite element model of the beam is used to analyze the effect of damage location and size on the mode shapes of the beam. The effect on mode shapes is amplified by the variation in the Fourier coefficients. It is found that damage location and size affects Fourier coefficients. The Fourier coefficients of the first three modes can be used to detect damage in the beam. It is also found that some Fourier coefficients are effective damage indicators even in the presence of noise. Hence, the proposed method can be used for detecting the damage in the beams simply supported at both ends with good accuracy.

References

Carden, E.P.; Fanning, P. (2004): Vibration based condition monitoring: A review, *Structural Health Monitoring*, Vol. 3, No. 4, pp. 355-377.

Chandrashekhar, M.; Ganguli, R. (2009): Damage assessment of structures with uncertainty by using mode-shape curvatures and fuzzy logic, *Journal of Sound and Vibration*, Vol. 326, No. 3-5, pp. 939-957.

Chang, C.C.; Chen, L.W. (2004): Damage detection of cracked thick rotating blades by a spatial wavelet based approach, *Applied Acoustics*, Vol. 65, No. 11, pp. 1095-1111.

Doebling, S.W.; Farrar, C.R.; Prime, M.B. (1998): A summary review of vibration-based damage identification methods, *The Shock and Vibration Digest*, Vol. 30, No. 2, pp. 91-105.

Douka, E.; Louridis, S.; Trochidis, A. (2003): Crack identification in beams using wavelet analysis, *International Journal of Solids and Structures*, Vol. 40, No. 13-14, pp. 3557-3569.

Fang, S.; Perera, R. (2009): Power mode shapes for early damage detection in linear structures, *Journal of Sound and Vibration*, Vol. 324, No. 1-2, pp. 40-56.

Gao,W. (2007): Natural frequency and mode shape analysis of structures with uncertainty, *Mechacial Systems and Signal Processing*, Vol. 21, No. 1, pp. 24-39.

Giridhara, G.; Gopalakrishnan, S. (2009): Frequency Domain based Damage Index for Structural Health Monitoring, *Structural Durability and Health Monitoring*, Vol. 5, No. 1, pp. 1-32.

Gokdag, H.; Kopmaz, O. (2009): A new damage detection approach for beam-type structures based on the combination of continuous and discrete wavelet transforms, *Journal of Sound and Vibration*, Vol. 324, No. 3-5, pp. 1158-1180.

Hong, J.C.; Kim, Y.Y.; Lee, H.C.; Lee, Y.W. (2002): Damage detection using the Lipschitz exponent estimated by the wavelet transform: applications to vibration modes of a beam, *International Journal of Solids and Structures*, Vol. 39, No. 7, pp. 1803-1816.

Lee, J. (2009): Identification of multiple cracks in a beam using natural frequencies, *Journal of Sound and Vibration*, Vol. 320, No. 3, pp. 482-490.

Loya, J.A.; Rubio, L.; Saez, J.F. (2006): Natural frequencies for bending vibrations of Timoshenko cracked beams, *Journal of Sound and Vibration*, Vol. 290, No. 3-5, pp. 640-653.

Mazanoglu, K.; Yesilyurt, I.; Sabuncu, M. (2009): Vibration analysis of multiple-cracked non-uniform beams, *Journal of Sound and Vibration*, Vol. 320, No. 4-5, pp. 977-989.

Morlier, J.; Bos, F.; Castera, P. (2009): Diagnosis of a portal frame using advanced signal processing of laser vibrometer data, *Journal of Sound and Vibration*, Vol. 297, No. 1-2, pp. 420-431.

Ostachowicz, W.M. (2008): Damage detection of structures using spectral finite element method, *Computers and Structures*, Vol. 86, No. 3-5, pp. 454-462.

Pandey, A.K.; Biswas, M.; Samman, M.M. (1991): Damage detection from changes in curvature mode shapes, *Journal of Sound and Vibration*, Vol. 145, No. 2, pp. 321-332.

Park, J.H.; Kim, J.T.; Hong, D.S.; Ho, D.D.; Yi, J.H. (2009): Sequential damage detection approaches for beams using time-modal features and artificial neural networks, *Journal of Sound and Vibration*, Vol. 323, No. 1-2, pp. 451-474.

Pawar, P.M.; Reddy, K.V.; Ganguli, R. (2007): Damage Detection in Beams Using Spatial Fourier Analysis and Neural Networks, *Journal of Intelligent Material Systems and Structures*, Vol. 18, No. 4, pp. 347-359.

Peng, Z.K.; Lang, Z.Q.; Chu, F.L. (2008): Numerical analysis of cracked beams using nonlinear output frequency response functions, *Computers and Structures*, Vol. 86, No. 17-18, pp. 1809-1818.

Poudel, U.P.; Fu, G.; Ye, J. (2005): Structural damage detection using digital video imaging technique and wavelet transformation, *Journal of Sound and Vibration*, Vol. 286, No. 4-5, pp. 869-895.

Qiao, P.; Cao, M. (2008): Waveform fractal dimension for mode shape-based damage identification of beam-type structures, *International Journal of Solids and Structures*, Vol. 45, No. 22-23, pp. 5946-5961.

Qiao, P.; Lu, K.; Lestari, W.; Wang, J. (2007): Curvature mode shape-based damage detection in composite laminated plates, *Composite Structures*, Vol. 80, No. 3, pp. 409-428.

Quek, S.T.; Wang, Q.; Zhang, L.; Ang, K.K. (2001): Sensitivity analysis of crack detection in beams by wavelet technique, *International Journal of Mechanical Sciences*, Vol. 43, pp. 2899-2910.

Raghuprasad, B, K.; Lakshmanan, N.; Gopalakrishnan, N.; Muthumani, L. (2008): Sensitivity of Eigen Values to Damage and Its Identification, *Structural Durability and Health Monitoring*, Vol. 4, No.3, pp. 117-144.

Ratcliffe, C.P. (1997): Damage detection using a modified Laplacian operator on mode shape data, *Journal of Sound and Vibration*, Vol. 204, No. 3, pp. 503-517.

Reddy, K.V.; Ganguli, R. (2007): Fourier Analysis of mode shapes of damaged beams, *Computers, Materials and Continua*, Vol. 5, No. 2, pp. 79-97.

Sawyer, J.P.; Rao, S.S. (2000): Structural damage detection and identification using fuzzy logic, *AIAA Journal*, Vol. 38, No. 12, pp. 2328-2335.

Sazonov, E.; Klinkhachorn, P. (2005): Optimal spatial sampling interval for damage detection by curvature or strain energy mode shapes, *Journal of Sound and Vibration*, Vol. 285, No. 4-5, pp. 783-801.

Shih, H.W.; Thambiratnam, D.P.; Chan, T.H.T. (2009): Vibration based structural damage detection in flexural members using multi-criteria approach, *Journal of Sound and Vibration*, Vol. 323, No. 3-5, pp. 645-661.

Sinou, J.J. (2009): Damage Assessment Based on the Frequencies' Ratio Surfaces Intersection Method for the identification of the Crack Depth, Location and Orientation, *Structual Durabilty and Health Montioring*, Vol. 3, No. 3, pp. 133-164.

Wang, B.S.; He, Z.C. (2007): Crack detection of arch dam using statistical neural network based on the reductions of natural frequencies, *Journal of Sound and Vibration*, Vol. 302, No. 4-5, pp. 1037-1047.

Whalen, T. M. (2008): The behavior of higher order mode shape derivatives in damaged beam-like structures, *Journal of Sound and Vibration*, Vol. 309, No. 3-5, pp. 426-464.

Yana, Y.J.; Cheng, L.; Wu, Z.Y.; Yam, L.H. (2007): Development in vibration based structural damage detection technique, *Mechanical Systems and Signal Processing*, Vol. 21, pp. 2198-2211.

Yoon, M.K.; Heider, D.; Gillespie, J.W.; Ratcliffe, C.P.; Crane, R.M. (2005): Local damage detection using the two-dimensional gapped smoothing method, *Journal of Sound and Vibration*, Vol. 279, No. 1-2, pp. 119-139.

Zhao, J.; Tang, J.; Wang, K.W. (2008): Enhanced statistical damage identification using frequency-shift information with tunable piezoelectric transducer circuitry, *Smart Materials and Structures*, Vol. 17, No. 6, pp. 12.

Zhao-de, Z.; Shuai, C. (2007): Crack detection using a frequency response function in offshore platforms, *Journal of Marine Science and Application*, Vol. 6, No. 3, pp. 1-5.

Zhong, S.; Oyadiji, S.O. (2008): Analytical prediction of natural frequencies of a cracked simply supported beams with a stationary roving mass, *Journal of Sound and Vibration*, Vol. 311, No. 1-2, pp. 328-352.

Zhong, S.; Oyadiji, S.O.; Ding, K. (2008): Response-only method for damage detection of beam-like structures using high accuracy frequencies with auxiliary mass spatial probing, *Journal of Sound and Vibration*, Vol. 311, No. 3-5, pp.1075-1099.

Zou, Y.; Tong, L.; Steven,G.P. (2000): Vibration-based model-dependant damage (delamination) identification and health monitoring for composite strctures - A review, *Journal of Sound and Vibration*, Vol. 230, No. 2, pp. 357-378.